haematologica
Journal of the Ferrata Storti Foundation

# Stem cell factor and erythropoietin-independent production of cultured reticulocytes

by Emmanuel Olivier, Shouping Zhang, Zi Yan, and Eric E. Bouhassira

*Received: October 13, 2023.*
*Accepted: April 5, 2024.*

*Citation: Emmanuel Olivier, Shouping Zhang, Zi Yan, and Eric E. Bouhassira.*
*Stem cell factor and erythropoietin-independent production of cultured reticulocytes.*
*Haematologica. 2024 Apr 11. doi: 10.3324/haematol.2023.284427 [Epub ahead of print]*

**Stem cell factor and erythropoietin-independent production of cultured reticulocytes**

Emmanuel Olivier[1], Shouping Zhang[1], Zi Yan[1], and Eric E Bouhassira[1]*

Department of Cell Biology, Albert Einstein College of Medicine

Bronx, New York, 10461

1: Department of Cell Biology, Albert Einstein College of Medicine, Bronx, New York, 10461

*: Correspond author: email: eric.bouhassira@einsteinmed.edu

Author contributions:

SZ and ZY performed experiments.

EO performed, designed and interpreted experiments.

EEB performed, designed and interpreted experiments, wrote the manuscript and supervised the study.

Disclosures: none of the authors have any disclosure.

Data sharing statement: Cells generated in these studies are available upon request.

**Abstract:**

Cultured reticulocytes can supplement transfusion needs and offer promise for drug delivery and immune tolerization. They can be produced from induced pluripotent stem cells (iPSCs), but the 45-day culture time and cytokine costs make large-scale production prohibitive. To overcome these limitations, we have generated IPSCs that express constitutive SCF receptor and jak2 adaptor alleles. We show that iPSC lines carrying these alleles can differentiate into self-renewing erythroblast (SRE) that can proliferate for up to 70 cell-doubling in a cost-effective, chemically-defined, albumin- and cytokine-free medium. These kitjak2 SREs retain the ability to enucleate at a high rate up to senescence. Kitjak2 derived cultured reticulocytes should be safe for transfusion because they can be irradiated to eliminate residual nucleated cells. The kitjak2 cells express blood group 0 and test negative for RhD and other clinically significant RBCs antigens and have sufficient proliferation capacity to meet global RBC needs.

**Introduction**

Cultured reticulocytes (cRetic), which can mature into red blood cells (RBCs) upon transfusion [1], have the potential to supplement transfusion needs, to be used as drug carriers or as immune tolerization agents [2] . Several methods have been devised to amplify primary cord blood (CB) or peripheral blood (PB) hematopoietic progenitor cells (HPCs) into cRetics [3, 4]. These processes involve multi-stage culture protocols during which the HPCs expand and differentiate into reticulocytes. Erythroid differentiation of HPCs is typically achieved using various combination of cytokines and small molecules, the most important being Stem Cell Factor (SCF), Erythropoietin (Epo), interleukin-13 and dexamethasone (Dex). These methods can achieve up to $10^5$-fold cell expansion of HPCs into cRetic and offer a potential solution to relieve local blood shortages. However, they are not ideal for large scale production of cRetics because the primary cells required for this process must constantly be replenished.

To overcome this limitation, several immortalized cell lines have been developed. This was achieved by lentiviral transduction of CB, PB or bone marrow (BM) CD34+ or mononuclear cells to overexpress the E6 and E7 proteins of human papilloma virus (HPV) 16 [5-9] , sometimes combined with hTERT or Simian Virus 40 T antigen [10]. Additionally, other erythroid cell lines have been generated by over-expression of cellular genes such as c-myc and Bcl-XL, Spi1 or Bmi-1 [11, 12].

Many of these lines can be cultured for months and in some cases indefinitely and exhibit a phenotype that resembles certain stages of red blood cell development, generally colony forming unit-Erythroid (CFU-Es) or pro-erythroblasts. Importantly, some of these cell lines retain the ability to differentiate into reticulocytes with rates of enucleation varying between <1% up to about 30%, even after long-term culture [5, 6, 13].

These cell lines are invaluable for research, particularly in studying the process of RBC formation. They also hold promise as a source of cells for blood transfusions and other applications involving cRetics. However, there are still challenges to be addressed. For instance, cell lines expressing the HPV E6/E7 proteins invariably show significant aneuploidy [5]. The cost of the culture media and cytokines needed to maintain these cells, and the low cell densities required for effective terminal differentiation are also hurdles that need to be overcome for these lines to be viable for large-scale RBC production for clinical use.

Induced pluripotent stem cells (iPSCs) present a viable alternative source for cRetic production because they are inherently immortal, maintain karyotypic stability and are easy to produce. Multiple labs have developed and refined protocols to differentiate iPSCs into cRetics, first using feeder layer and then using feeder-free protocols [14, 15]. These experiments revealed that the cRetics derived from iPSCs predominantly expressed embryonic and fetal globins rather than the adult variant and are larger in size than typical adult RBCs. [16]

In an effort to decrease the cost of cRetics production from iPSCs, we previously developed two chemically defined cul-

ture media, IMIT and R6, and combined them into Pluripotent Stem Cell Robust Erythroid Differentiation (PSC-RED) protocols which yield, in its long version, more than 100,000 cRetics / iPSC [17]. A notable feature of PSC-RED is its elimination of the need for albumin and a significant reduction in transferrin requirements—by twentyfold compared to previous methods. This efficiency is due to an iron chelator in the R6 media, which facilitates transferrin recycling in the cell culture.

However, despite these improvements, the PSC-RED protocol proved in our hands to be too expensive and too complex for large scale production. This is partly due to the lengthy differentiation process of iPSCs into cRetics, which takes 40 to 45 days, and partly because of the high costs of SCF and Epo.

Independent of the cell source used, producing a single unit of RBCs containing $2x10^{12}$ cells theoretically requires over 1,000 liters of medium in a static culture system where the maximum cell density is approximately $2x10^{6}$ cells/mL. Since these large volumes are unpractical and prohibitively expensive, investigators have sought to overcome these limitations by growing the cells in bioreactors which can theoretically support a much higher cell density. Griffith et al. were able to produce $3.10^{10}$ cRetics (about 5 mL of packed cells) in 24 liters at a density of $1\text{-}6.10^{6}$ cells/mL using a 2 liters stirred glass bioreactor [18]. A more recent study based on measurements of erythroblast $O_2$ uptake rate suggested that density greater than $10^{9}$ cells/mL might be achievable and that 500 liters of medium might be sufficient to produce 1 unit of cRetics [19]. Sivalingam et.al. were able to achieve complete differentiation of IPSCs into cRetics in a perfusion bioreactor, reaching a cell density of $3.5x10^{7}$/mL [20]. Others studies have reported achieving very high cell densities using various small scale 3D bioreactor designs (reviewed in [21]). Collectively, these findings suggest that large scale production of cRetics is technically possible with existing bioreactor technology. However, each cell sources comes with inherent limitations and the high costs associated with these processes currently impede the widespread production of cRetics for transfusion.

In the case of the PSC-RED protocol, about seventeen liters of culture medium are consumed during the 45-day PSC-RED protocol to produce $5.10^{9}$ cRetics, the equivalent of about 1 ml of blood. However, less than 50 mL of medium is consumed during the first 17 days because of the exponential proliferation of the cells (**Figure S1).** Most of the cost of cRetic production is therefore incurred after day 17. Since SCF and Epo are the only cytokine required after day 17, we decided to test the hypothesis that the introduction of constitutive mutations in the SCF and Epo pathways would allow us to produce cRetics from iPSCs without SCF or Epo.

To test this hypothesis, we selected the kitD816V mutation, often associated with mastocytosis, because it causes the kit gene (the SCF receptor) to become constitutively active [22]. Additionally, we chose the jak2V617F, frequently associated with polycythemia vera (PV), because it significantly reduces the need for Epo by enabling the jak2 kinase to signal in the absence of this cytokine. [23] The selection of the kitD816V mutation was supported by a report indicating that the Epo- and SCF-dependent HUDEP-2 transformed erythroid cell line, [13] could be rendered independent of SCF by introducing mutations around position 816 of the kit gene. [24]. Importantly, the Epo dependence of some HUDEP-2 sub-lines described in this report was also reduced, possibly due to interactions between the SCF and Epo receptors. [25]

We report that iPSC lines carrying these alleles can differentiate into self-renewing erythroblast (SRE) that can proliferate for up to 70 cell-doubling in a cost-effective, chemically-defined, albumin- and cytokine-free medium. These kitjak2 SREs are karyotypically stable and retain the ability to enucleate at a rate > 50%. The development of these Kitjak2 SREs removes major obstacles to the production of large amounts of cRetics for translational applications.

**Methods:**

**Internal Review Board:** All experiments involving human cells were performed under a protocol approved by the Albert Einstein College of Medicine IRB (Bronx, New York).

**Induced-pluripotent stem cells:** iPSCs line O1 and O2 have been described previously [17].

**Self-renewing erythroblasts:**

**Differentiation of iPSCs into kitjak2 SREs:**

**Day 0**: kitjak2 iPSCs were differentiated into day-17 HPCs according to the PSC-Red protocol (omitting SCF)

**Day 17:** day-17 HPCs were then cultured in IMIT combined with 1mM Dex, 30mM IBMX. After 10 to 14 days, greater than 98% of the cells in the culture had acquired the antigen profiles of SREs.

**Differentiation of iPSCs into kitD816V SREs.**

**Day 0**: kitD816V iPSCs were differentiated into day-17 HPCs according to the PSC-Red protocol (omitting SCF)

**Day 17:** day-17 HPCs were then cultured in IMIT combined with 1mM Dex, 30mM IBMX and 1u/mL Epo. After 10 to 14 days, greater than 98% of the cells in the culture had acquired the antigen profiles of SREs.

**Long-term culture of SREs:** kitjak2 SREs can be cultured for about 120 days in IMIT combined with 1uM Dex and 30uM IBMX. D816V SREs can be cultured for about 140 days in in IMIT combined with 1uM Dex, 30uM IBMX and 1 u/mL of Epo. They can also be cultured for about 45-55 days in the same medium without Epo.

All SREs were passaged every 3 to 5 days by dilution to 1.25 to 2.5x$10^5$ cells/mL once the culture concentration exceeded 1.5x$10^6$/mL. The passage frequency depended on the passage number because the rate of proliferation of the SREs diminishes gradually over time.

**Terminal differentiation of SREs:**

**Day 0:** Cells were centrifuged, rinse once in PBS to eliminate all traces of Dex and IBMX and plated at about 1.5x$10^5$ cells/mL in R6 media containing 4U/ml of Epo, and 5% human AB plasma and 1mM RU 486

**Day 3**: Cells were diluted 1 to 2 to about 3.5x$10^5$ cells/mL in the same media without Epo.

**Days 5, 7 and 9:** Cells were diluted in pure RPMI to about 3 to 5x$10^5$ cells/mL.

**Flow cytometry:** iPSCs undergoing differentiation were evaluated by FACS using a Cytek aurora spectral cytometer and a 15-color antibodies panel described in **Table S3**. Data were analyzed with the FlowJo software using the FlowSOM [26] and UMAP [27] plugins, essentially as suggested by the manufacturer using the default parameters.

**Low-pass sequencing:** Genomic DNA was extracted and 1.5Gb of sequence was obtained on an Illumina sequencer (2x150bp configuration). Reads were aligned to the hg38 genome using the bwa aligner and copy-number variants were detected using the CNVKit software package [28]. A library of 10 normal genomes sequenced to the same depth was used as a baseline control. iPSCs genomic DNA were also compared with the DNA obtained from peripheral blood cells from the same donor.

**Reagents:** The suppliers for all reagents are provided in **Table S5**.

**Statistical analysis:** Paired and unpaired t-tests were used to assess significance using the GraphPad Prism software.

Detailed protocols for other procedures are provided as supplementary materials.

**Results:**

**Production of iPSCs carrying the D816V mutation.** To generate cells with the kitD816V mutation, we transfected the iPSC clone O1 [17] with cas9 mRNA, an sgRNA targeting exon 17 of the kit gene, and a 200 bp homology-directed recombination (HDR) donor oligonucleotide. Screening 24 iPSC clones showed a targeting frequency of about 50% (**Figure S2**). We selected lines homozygous (B34) and hemizygous (A4) for the D816V mutation for further characterization.

**cRetics can be produced without SCF.** During the PSC-RED protocol, iPSCs differentiate into cRetics over a period of 45 days. Initially, from day 0 to day 17, the cells are sequentially cultured with four supplements (S1 to S4), resulting in a mixture of HPCs (**Figure 1A**). These HPCs are then directed towards early erythroid differentiation by being cultured in the presence of Stem Cell Factor (SCF), erythropoietin (Epo), dexamethasone (Dex), and 3-Isobutyl-1-methylxanthine (IBMX) between days 17 and 24. From days 24 to 38, the cells progress to the late erythroid stage when maintained in similar media, but without Dex or IBMX. In the final phase, these late-stage progenitors mature and enucleate when cultured from day 38 to 45 without any cytokines or small molecules.

To evaluate the phenotype of the kitD816V iPSCs, we differentiated the A4, B34, and the unedited O1 iPSC lines using the PSC-RED protocol but omitting SCF, which is normally present from day 2 to 38, at all steps of the protocols (**Figure 1A**). As anticipated, the unedited O1 iPSCs could not survive beyond day 17 in the absence of SCF (data not shown). In contrast, the A4 and B34 lines grew exponentially and exhibited a viability (assessed weekly using staining with propidium iodide) greater than 90% during the entire growth period, generating over 200,000 cells/ iPSC by day 38. Viability and yield were comparable to the cell production from control O1 iPSCs differentiated in the presence of SCF (**Figure 1B, black curve**).

Analysis of the cells generated in these cultures through Romanowsky staining, a stain similar to Giemsa, (**Figure S3**)

revealed that the kitD816V iPSCs acquired a progressively mature erythroid phenotype during the differentiation process. Analysis through a 15-color flow cytometry assay demonstrated that the progression of cells during the PSC-RED protocol could be succinctly represented using the flowSOM and UMAP algorithms [29, 30]. These algorithms categorized the cells into four distinct populations of HPCs (HPC1 to HPC4) and four populations of erythroid cells (Ery1 to Ery4), based on the expression patterns of ten surface antigens (**Figures 1C-E and S4A and S4C**).

Examination of the data revealed that the erythroid populations became predominant earlier in the differentiation process in the presence of the kitD816V mutation than in the control cells. Multiple hypotheses might explain this observation. One possibility is that the constitutive activation of the SCF signaling pathways in the D816V cells allows the proliferation of early primitive HPCs and erythroid cells that do not proliferate in the absence of the kit mutation because of the relatively low concentration of SCF (10ng/mL) and the absence of Epo during the first 17 days of the PSC-RED protocol.

To gain further insight into the differentiation potential of the iPSC-derived HPCs in the presence of the kit mutations we performed methyl-cellulose assays on cells obtained at days 10, 17 and 24 of the PSC-RED protocol. Control O1 cells were obtained in the presence of SCF, but this cytokine was omitted when generating the cells from the kit mutated A4 and B34 iPSCs (**Figure S5**). For all three iPSC lines tested, the proportion of clonogenic cells was highest at day 10 and gradually decreased until day 24 (averaging 772 ± 92 / 10,000 HPCs at day 10, 162 ± 196 / 10,000 HPCs at day 17 and 70 ± 23 / 10,000 HPCs at day 24). Notably, both myeloid and erythroid colonies were obtained at all time points, the number of colony-forming-unit granulocyte, erythrocyte, monocyte, megakaryocyte (CFU-GEMM) colonies decreased over time while the ratio of colony-forming-unit-erythroid (CFU-E) to burst-forming-unit-erythroid (BFU-E) increased. No significant difference in the distribution of the colonies between the control and kitD816V cells was observed.

Upon completion of the differentiation process, the hemizygous kitD816V A4 clone yielded a combination of basophilic erythroblasts (referred to as Ery3), orthochromatic erythroblasts, and enucleated cells (referred to as Ery4), a pattern similar to that of the control cells. In the case of the homozygous (B34) clone, the erythroid populations proliferated even earlier than those of the A4 clone. In addition, the B34 clone generated Ery3 cells but few Ery4 cells. Repeat of this differentiation experiment using new batches of antibodies confirmed that the erythroid cells dominated the culture earlier in the presence of the D816V mutations than in the control cells, and that the B34 iPSCs produced fewer Ery4 cells than the A4 iPSCs (**Figure S4B)**.

**Epo is also dispensable for the production of iPSC-derived kitD816V erythrocytes.**

To investigate the potential of iPSC-derived kitD816V cells to differentiate in the absence of both Epo and SCF, we induced the differentiation of the A4 and B34 iPSC lines omitting both cytokines (**Figure 2A**). This demonstrated that both lines could proliferate without Epo and SCF yielding a substantial number of cells (>200,000 cells/iPSC). Again fewer Ery4 cells were produced by the B34 clones than by the control and A4 clones (**Figure 2B-B34C**).

**KitD816V cRetics express mostly fetal globins.** To measure the enucleation rate, day-45 cells cultured without SCF

and induced to terminally differentiate by discontinuing Epo on day 38 were analyzed by flow cytometry after staining with Draq5, a cell permeant DNA dye, and by light-microscopy following Romanowsky staining. To test the hypothesis that in this system constitutive activation of the SCF receptor might be detrimental to terminal erythroid differentiation, we also investigated the potential of dasatinib [31], an inhibitor of the kinase activity of the kitD817V SCF receptor, to enhance terminal differentiation.

In the absence of dasatinib, the enucleation rate of A4 cells averaged 14.65 ± 4.4%, similar to the control cells. This rate rose to 21.8 ± 4.9 when 200nM of dasatinib was added on day 31 (**Figure 3A**). Further analysis of Romanowsky-stained microscope slides revealed that dasatinib also accelerated the differentiation process (**Figures 3B-C**). Subsequently, the globin chain composition of cells obtained on day 45 was analyzed through reverse-phase HPLC. As previously reported [17], reticulocytes and orthochromatic erythroblasts produced from the control O1 cells expressed mostly fetal γ-globin chains (**Figure 3D**). Cultured RBCs obtained from the A4 line also expressed predominantly fetal γ-globin, alongside detectable embryonic globin chains. Further experiments indicated that A4 cells grown without SCF and Epo enucleated at similar rates (data not shown).

**The impact of the kitD816V mutation on erythroid differentiation can be replicated in iPSCs from a distinct donor.** To replicate these findings and assess the phenotype of heterozygous kitD816V iPSCs (which were not obtained in the experiments described above), CRSPR editing was repeated on cells from two donors (O1 and O2), mixing in an additional HDR donor oligonucleotide encoding the wild-type sequence in equal proportions with the kitD816V HDR oligonucleotide. This approach yielded multiple clones heterozygous for the D816V mutation for both the O1 and O2 donors (**Figure S6A**). Differentiation experiments using the PSC-RED protocol revealed that these clones proliferated at a high rate (slightly lower than the A4 hemizygous clones) and could produce enucleated cells (**Figures S6B-C**). These results indicate that the kitD816V mutation represents a reliable and broadly applicable approach to generate iPSC lines capable of differentiating into RBCs without the need for SCF.

**Production of SCF independent self-renewing erythroblasts.** It has long been known that the glucocorticoid receptor is a key regulator of the decision between self-renewal and differentiation in erythroid progenitors and that both human and mouse CFU-E/pro-erythroblasts can self-renew for a limited time when cultured in the presence of SCF, Epo and Dex [4, 32, 33]. In addition, we have previously shown that erythroblasts derived from human pluripotent stem cells could self-renew in culture for an extended period of time in the presence of the same factors [14]. To investigate whether kitD816V erythroid progenitors also exhibit self-renewal capabilities, we used the PSC-RED protocol to generate day-17 HPCs from the A4 and B34 iPSCs lines and expanded them without cytokines but with Dex and IBMX (referred to as DI conditions). Both lines demonstrated the ability to expand under these conditions for approximately 45 to 55 days resulting in a greater than 1,000-fold expansion before reaching a plateau and ceasing to proliferate (**Figure 4B**). Flow cytometry analysis indicated that in the DI conditions the A4 and B34 day-17 HPCs downregulated CD49f, CD45, CD38 and CD34 and upregulated expression of CD36, CD71, and CD235a (**Figure S7A**). This transition from an HPC to an erythroblast phenotype, resembling iPSC-derived late CFU-Es and pro-erythroblasts, was almost completed by day 24. After

that time point the antigen profiles of both the A4 and B34 cells remained constant, suggesting that the cells were self-renewing. Romanowsky staining supported these findings since it showed that the kitD816V d17-HPCs cultured in DI conditions exhibited a very uniform CFU-E/pro-erythroblast phenotype at day 45 (**Figure S7B**), while the same day-17 HPCs cultured according to the PSC-RED protocol differentiated into orthochromatic erythroblasts and reticulocytes (**Figures S3B and C**). We concluded from these experiments that kitD816V day-17 HPCs were able to differentiate into erythroblasts with limited self-renewing capability when grown in the absence of SCF and Epo.

Since the A4 cells were easier than the B34 cells to differentiate, we focused subsequent experiments on the former cells. Crucially, further experiments, indicated that adding 1 unit / mL of Epo to Dex and IBMX (referred to as EDI conditions) enabled the A4 erythroblasts to proliferate without differentiation for over 25 passages (approximately 120 days), resulting in a $10^{20}$-fold amplification (**Figure 4C**). Remarkably, the viability of these SREs, assessed by propidium iodide or by Annexin V staining, during this expansion phase was between 90 and 99% at all times (**Figure S8**). These findings indicated that self-renewing erythroblasts (SREs) capable of sustained growth without the need for SCF can be generated from kitD816V iPSCs.

**Production of SCF and Epo independent kitjak2 SREs**. To investigate the possibility of obtaining cells capable of a similar long-term self-renewal without requiring Epo, we introduced the jak2V617F mutation through CRSPR-mediated mutagenesis in the A4 line using the method described earlier. Once again, over 50% of the screened clones had acquired the Jak2V617F mutation (**Figure S9A and B)**. We termed the double-mutant, the kitjak2 lines. When subjected to differentiation using the PSC-RED protocol, iPSC lines hemizygous for the kitD816V mutation and either homozygous (lines G19 and H12) or hemizygous (lines H5 and H11) for the jak2V617F mutation demonstrated the ability to undergo erythroid expansion and differentiation in the absence of both SCF and Epo (**Figure 4D and S9C**).

Significantly, additional experiments demonstrated that day-17 HPCs from the G19 and H12 kitjak2 SREs cultured in Dex + IBMX (DI conditions) proliferated exponentially in the absence of SCF and Epo for about 3 months before entering a state of senescence, suggesting that they had differentiated into SREs. Even more remarkable, the H5 and H12 cells proliferated in the same conditions for more than 4 months resulting in an amplification of greater than $10^{18}$-fold (**Figure 4E**). Similarly to the A4 cells grown in EDI conditions, propidium iodide staining revealed that the viability of the kitjak2 SREs grown in DI conditions was very high (90-99%) until senescence (**Figure S8**). Flow cytometry analysis confirmed that the A4 and kitjak2 SREs cultured in DI conditions, rapidly acquired a phenotype almost identical to the SRE phenotype of the A4 cells grown in EDI conditions (**Figure 4F and S10AB**). Again, the transition between the d17-HPC phenotype and the SREs phenotype was almost completed by day 24 and became stable after day 31 of culture. Remarkably, the antigen profile of all the SREs analyzed was strikingly similar and varied minimally over a span of seventy days. Romanowsky-staining performed at early and late passages, revealed that all the SREs exhibit a uniform CFU-E/pro-erythroblasts erythroid morphology, with few signs of differentiation, confirming the FACS data (**Figure S7 and S10C**).

**Kitjak2 cells can differentiate into cRetics after extended culture without cytokines.** To investigate the potential of the A4 and kitjak2 SREs respectively expanded in EDI and DI conditions, we initiated their differentiation by withdrawing

Epo, Dex and IBMX from the culture media. This resulted in a rapid seven-day differentiation which produced a few enucleated cells, but with a yield of cRetic / SREs of only about 0.1 to 0.01 due to high cell mortality (data not shown).

Epo serves as the primary cytokine shielding erythroblasts from apoptosis [34]. To enhance the differentiation of these cells, we administered a pulse of Epo (4u / mL) to cushion the cells from the abrupt withdrawal of Dex and IBMX, and supplemented with 5% human plasma during the initial five days of differentiation (**Figure 5A**). These adjustments dramatically improved survival and lengthened the differentiation period to between 9 and 11 days. For both the A4 and the kitJak2 SREs, the cells expanded about 30 to 40-fold during the differentiation period (**Figure 5B and S11A and S12**). Viability, assessed by propidium iodide and acridine orange staining on a Luna FL cell counter, was above 95% between day 3 and day 9 (**Figure 5B**). Viability on day 11 was lower but varied between experiments. Together, these results suggest that the cells divided at least 5 times during the differentiation period.

FACS analysis revealed that expression of the CD235a antigen, which was expressed in almost all cells throughout the differentiation period, increased as the cells progressed toward terminal maturation (**Figure 5C, and S11A**). In contrast, CD43 expression, an antigen recently identified as useful to assess erythroid differentiation in iPSCs [35], was present on almost all cells at days 3 and 6 but was nearly completely silenced by day 9. Similarly, CD36 expression decreased over time but its silencing occurred later than that of CD43. Finally, CD71, one of the last markers to be silenced during erythroid differentiation, also followed the expected pattern of expression, though its silencing was not as complete as that of the other markers, possibly because our culture conditions are not optimal for reticulocyte maturation. Romanovsky staining confirm the FACS analysis, with pro- and basophilic erythroblasts abundant during the initial days of differentiation, and polychromatophilic, orthochromatophilic erythroblasts and reticulocytes dominating during the final days (**Figure 5D and S11B**). The overall patterns of differentiation were very similar for the A4 SREs and for the H5 kitJak2 SREs (**Figure S11C-E**).

To further examine the viability, we stained A4 and H5 kitJak2 SREs with Annexin V-FITC and DAPI and monitored apoptosis by FACS from days 3 to 11 (**Figures 5E and S11D and S12**). This analysis revealed that the proportion of annexin V positive apoptotic cells ranged from 11% to 16% between days 3 and 9, confirming the cells' high viability during differentiation. At day 11, the percentages of apoptotic cells were significantly higher and more variable across experiments, aligning with the results obtained with propidium iodide staining.

Staining with Draq5 and FACS analysis showed that the rate of enucleation varied from 30 to 55% averaging about 30% for the A4 lines and more than 50% for the H5 SREs (**Figure 5F**). On average, cell amplification during terminal differentiation, based on more than 10 experiments, exceeded a 30-fold increase for the A4 line and reached about 28-fold for the H5 line. This resulted in a yield of more than 10 reticulocytes per A4 or H5 SREs plated on day 0 (**Figure 5F**). Determining the optimal day for harvesting the cRetics proved challenging, because the rate of enucleation tended to increase between day 9 and 11, but in some experiments the viability of the cells decreased dramatically at either day 10 or 11. Additional experiments revealed that both the A4 and all kitjak2 SREs that we generated could differentiate into cRetics up to the point of senescence (**Figure S13**).

**Characterization of the cRetics derived from the A4 and kitjak2 cells.** To evaluate the quality of the RBCs originating from the A4 and the kitjak2 self-renewing erythroblasts, we purified enucleated cells using PALL Acrodisc filters. We then generated HPLC globin profiles and gathered morphological data via light microscopy, and red cell indices with the Advia 2120 blood count analyzer. The purified RBCs expressed 78-82% fetal (Aγ and Gγ), 12-17% embryonic (ε) and 5 to 7 % adult (β) β-like globins. They also expressed trace amounts of embryonic (ζ) α-like globins (**Figure 5G**). Morphologically the cells were larger than standard adult RBCs (MCV of about 125fL vs 85 fL, and diameter of about 10.5um vs 8.3um) and were well hemoglobinized since they exhibited hemoglobin concentrations similar to control cells (about 28g/dL) (**Figure 5H)**.

**Karyotypic stability.** To examine if the kitD816V and jak2V617F mutations induce karyotypic instability or aneuploidy, we compared chromosome copy-numbers in SREs at passage 20 to 22 and in iPSCs at passage 38-40, before and after CRSPR/cas9 editing through low-pass whole-genome sequencing, using O1 and O2 donor-derived PB mononuclear cells as controls. Analysis with the CNVKit software [28] showed no detectable copy-number variations in any cell line studied while confirming the marked aneuploidy of control transformed cells sequenced at an equivalent depth (**Figures 6 and S14**). We concluded that cells carrying both the kitD816V and jak2V617F can be propagated in culture for long periods of time without acquiring karyotypic abnormalities.

**Reagent RBCs.** One application of cRetics is the production of reagent RBCs for identifying allo-antibodies in chronic transfusion recipients [36], minimizing transfusion reactions. Reagent cells typically come from volunteer blood, but there are shortages of cells to detect allo-antibodies in sickle cell anemia and myelodysplastic patients who constitute over 80% of all allo-immunized individuals at most blood banks. To investigate whether cRetics could fill this role, we tested whether we could detect Rhesus C, c, E, and e antigens on the surface of A4 cRetics using a solid phase red cell adherence assay [37]. This indicated that 5 million RBCs per test could be used to identify all four antibodies (**Figure 7**), demonstrating that cRetics produced without cytokines can be used as reagent RBCs.

**Discussion**

Our findings highlight the profound influence of constitutive alleles of the kit and jak2 genes on the erythroid differentiation of iPSCs. The kitD816V mutation completely alleviated the need for SCF and Epo, as all iPSC lines that we generated, regardless of genotype, were able to proliferate and differentiate into erythroblasts in the absence of these cytokines at about the same rate as control cells in the presence of cytokines. Homozygosity for the kitD816V partially hindered terminal erythroid differentiation, but hemizygous and heterozygous variants underwent terminal differentiation and showed high enucleation rates. iPSCs with both the kitD816V and jak2V671F mutations also thrived and differentiated without any cytokines, often surpassing control cells supplemented with SCF and Epo.

The kitD816V and jak2V671F allowed iPSCs to differentiate into erythroid cells in the absence of any cytokines starting at day 17 (**Figure 4D**). In additional experiments (not shown), we also observed that day 10-HPCs cultured according

to the short version of the PSC-RED protocol in which the expansion step from day 10 to 17 is omitted (**Figure 1A**), could also differentiate into mature erythroid cells in the complete absence of cytokine. These data show that the signaling pathways activated by the SCF receptor, which is known to interact with the Epo receptor [25] is necessary and sufficient to specify the erythroid differentiation of day-10 HPCs, at least in the presence of IBMX and dexamethasone.

Using flow-cytometry, we identified eight distinct cell populations through dimension reduction tools, flowSOM and UMAP. These groupings align reasonably well with the known sequence of antigen profiles during iPSC differentiation into hematopoietic and erythroid lineages. However, iPSC-derived erythropoiesis is complex because developmental hematopoiesis occurs in successive primitive, erythro-myeloid, and definitive waves, each linked to the production of specific globins [16]. As such, our defined populations likely encompass significant developmental heterogeneity because the markers we employed don't sharply distinguish between primitive and definitive erythroid cells. Consequently, the cRetics that we generated are probably a blend of primitive erythroid cells, which express embryonic and fetal globins, and more advanced fetal-like cells that exhibit both fetal and adult globins.

The key discovery presented here is that SREs can reproducibly be generated from iPSCs carrying the kitD816V and jak2V671F mutations. While the single-mutant kitD816V cells exhibited modest self-renewal—lasting approximately 50 days without cytokines—their proliferation potential surged to 140 days in the presence of Epo. Most remarkably, double-mutant kitjak2 cells thrived for about 120 days sans cytokines.

All of the SRE cultures that we developed, proliferated with a high viability, little signs of differentiation, retained the ability to enucleate at a high rate up until senescence, and could be consistently passaged at ratios from 1:10 to 1:15 every 3-4 days, utilizing a cost-effective, chemically-defined, albumin-free medium supplemented with a minimal amount of recombinant transferrin.

The self-renewal of kitjak2 cells hinges on the inclusion of two specific small molecules, Dex and IBMX. Dex is essential for the self-renewal of the A4 and kitjak2 self-renewing erythroblasts since withdrawal of this molecule leads to rapid differentiation. Dex has long been known to control erythroblast self-renewal, but its mechanism of action in erythropoiesis remains only partially understood [38]. Ashley et al. have recently shown that erythroid cultures of adult but not cord blood human $CD34^+$ cells are sensitive to Dex. [39] Furthermore, Dex treatment was found to result in the expansion of immature colony-forming unit–erythroid (CFU-E) populations, likely through the upregulation of p57Kip2. The observed lack of Dex sensitivity of human cord blood progenitors reported by Ashley, contrasts with findings in mice, where both fetal liver BFU-Es and CFU-Es have been shown to respond to Dex [40, 41]. Further studies will be necessary to determine if p57Kip2 plays a role in the self-renewal of the kitjak2 cells or if other mechanisms are involved.

IBMX, a non-specific inhibitor of cAMP and cGMP phospho-diesterases, elevates intracellular cAMP levels [42]. We incorporated IBMX in the PSC-RED protocol because high cAMP concentrations facilitate early HPC specification [43, 44]. IBMX also regulates erythropoiesis. The EpoR doesn't directly control cAMP, but agents such as forskolin and prostaglandins which modify cAMP concentration, do influence Epo-mediated erythropoiesis [45]. Notably, cAMP-inducing agents have

been shown to amplify the proliferation of colony-forming erythroid progenitors [46, 47]. We found that IBMX is essential for the self-renewal of A4 and kitjak2 erythroblasts, as its omission markedly reduced their proliferation and viability (data not shown). Understanding how kitD816V, Jak2V617F, Dex and IBMX jointly extend the self-renewal of kitjak2 cells will require additional studies.

The generation of kitjak2 cells is reproducible, as we successfully produced multiple lines from two distinct donors. SREs differentiate from iPSC-derived day 17-HPCs in less than two-weeks. This contrasts with immortalization using the HPV E6/E7 proteins which demands several months of transduced cell cultivation before cell lines emerge [5]. This reproducibility, paired with the rapid differentiation, indicates that no additional genetic or epigenetic alterations, beyond our engineered modifications, are necessary for the erythroblasts to achieve self-renewal without cytokines.

The cell lines that we generated are diploid and appear karyotypically stable likely because mutations in cytokine receptors and signaling adaptors don't directly drive chromosomal instability. Cultured RBCs derived from the kitjak2 lines should be safe for transfusion applications, despite the association between several malignancies and the kitD816V and jak2V617F alleles, because RBCs lack nuclei, and because any residual nucleated cells can be killed by irradiation [48].

Expression of JAK2 V617F in mouse fetal liver triggers activation of Stat5, the STAT normally activated by Epo, but also activates Stat1 and Stat3 [49]. In humans, the Jak2 V617F allele is associated with PV but can also cause essential thrombocythemia. By contrast, mutations in Jak2 exon 12, which are much rarer than the V617F mutation, are much more specifically associated with PV. Experiments in which both mutations have been introduced in iPSCs have shown that, compared with JAK2V617F-iPSCs, JAK2exon12-iPSCs produced a greater number of erythroid cells that displayed more mature morphology and expressed more adult hemoglobin [50]. Importantly, exon12 mutations led to significantly higher levels of phospho-STAT1 but lower phospho-STAT3 s compared with JAK2V617F-iPSCs in response to erythropoietin. These studies suggest that ectopic STAT1 activation plays a role in PV in humans. Whether stat1 and stat3 are activated in humans kitJAK2 SREs is currently unknown. Additionally, these data suggest that combining a Jak2 exon 12 and the KitD816V mutations might offer an alternative method for producing cytokine-independent SREs.

Differentiating a single iPSC using the PSC-RED protocol generates about $10^3$ day-17 HPCs. Each of these HPCs can produce about $10^{18}$ kitjak2 self-renewing erythroblasts, which each yield up to 10 RBCs. Thus, theoretically, a single iPSC is sufficient to produce the number of RBCs present in $>10^9$ liters of blood ($10^{21}$ cells), surpassing the global annual transfusion volume. Cytokine-independent SREs, such as those from the O1 and O2 donors, who have blood group 0 and test negative for RhD and other clinically significant RBCs antigens (**Figure 7B**), therefore have ample proliferation capacity to meet the needs for the foreseeable future.

Although the culture of iPSCs and the generation of day-17 HPCs remain costly, it's important to recognize that over 99% of the cell expansion needed for cRetics production from kitjak2 cells occurs at the SRE stage, using a cost-effective culture medium. Consequently, the cost of producing day-17 HPCs constitutes only a minor fraction of the overall expense in cRetics production.

Contrary to cells immortalized with HPV16 E6/E7 protein overexpression, kitjak2 SREs do not grow indefinitely. However, this isn't a significant concern since new, genetically identical kitjak2 SREs can be readily produced from iPSCs. More importantly, the approval of cRetics for clinical use by regulatory authorities, when derived from late passage cells after extensive proliferation, remains uncertain because prolonged cell division inevitably leads to the accumulation of harmful mutations. The capacity of kitjak2 SREs to undergo over 70 population doublings is adequate to produce large quantities of cRetics. Enhancing their proliferative capacity beyond this point may not be beneficial for their clinical application.

Kim et al. [51] in mice, and Liu et al. [52] in humans demonstrated that overexpressing the transcription factor Bmil, part of the polycomb group complex 1, in HPCs can produce adult SREs. These SREs can expand up to $10^{12}$ times in the presence of SCF, Epo, and Dex, while still retaining the capacity to differentiate into cRetics. This overexpression of Bmil presents a promising alternative for cRetic production. An advantage of this method is the potential for Bmil cRetics to express higher levels of adult globins compared to kitjak2 cRetics, although the HPLC globin profile of Bmil cRetics is not yet reported. In contrast, kitjak2 cRetics have the benefit of growing without cytokines and originating from immortal iPSCs.

A limitation of the kitjak2 cells is their fetal/embryonic characteristics, including their larger size compared to adult cells and predominant expression of Hb F. However, Hb F expression does not pose a concern for certain uses of cRetics. For instance, for drug delivery and reagent RBCs applications, where oxygen transport isn't the primary function of the cRetics, the type of hemoglobin expressed is not a major factor. Additionally, in transfusions for premature infants, an increasingly common procedure, Hb F expression can be beneficial, because it might prevent retinopathies [53]. Yet, for adult transfusion, Hemoglobin A is preferable. Therefore, different cell sources for cRetics production may be better suited for specific translational applications.

A detailed characterization of the kitjak2 cRetics will be necessary before testing these cells in clinical trials. Like all enucleated erythroid cells created *in vitro*, kitjak2-derived enucleated cells are reticulocytes, not mature RBCs. While transfused cRetics have been shown to mature into RBCs in vivo [1] , it would be interesting to explore if cRetics can mature into RBCs *in vitro,* considering the lack of established storage methods for cRetics.

In summary, we have developed a novel approach to produce cRetics from iPSCs which is more practical and most cost effective than previous approaches. The ability of kitjak2 iPSCs to differentiated into SREs that are karyotypically stable, can proliferate for up to 4 months in a cost-effective, chemically-defined, albumin- and cytokine-free cell culture medium, and that retain the ability to enucleate at a high rate should facilitate the production of cRetics for translational applications.

**References**


1. Kupzig S, Parsons SF, Curnow E, Anstee DJ, Blair A. Superior survival of ex vivo cultured human reticulocytes following transfusion into mice. Haematologica. 2017;102(3):476-483.
2. Villa CH, Cines DB, Siegel DL, Muzykantov V. Erythrocytes as Carriers for Drug Delivery in Blood Transfusion and Beyond. Transfus Med Rev. 2017;31(1):26-35.
3. Giarratana MC, Kobari L, Lapillonne H, et al. Ex vivo generation of fully mature human red blood cells from hematopoietic stem cells. Nat Biotechnol. 2005;23(1):69-74.
4. Migliaccio G, Sanchez M, Masiello F, et al. Humanized culture medium for clinical expansion of human erythroblasts. Cell Transplant. 2010;19(4):453-469.
5. Kurita R, Funato K, Abe T, et al. Establishment and characterization of immortalized erythroid progenitor cell lines derived from a common cell source. Exp Hematol. 2019;69:11-16.
6. Trakarnsanga K, Griffiths RE, Wilson MC, et al. An immortalized adult human erythroid line facilitates sustainable and scalable generation of functional red cells. Nat Commun. 2017;8:14750.
7. Cervellera CF, Mazziotta C, Di Mauro G, et al. Immortalized erythroid cells as a novel frontier for in vitro blood production: current approaches and potential clinical application. Stem Cell Res Ther. 2023;14(1):139.
8. Akimov SS, Ramezani A, Hawley TS, Hawley RG. Bypass of senescence, immortalization, and transformation of human hematopoietic progenitor cells. Stem Cells. 2005;23(9):1423-1433.
9. Malagutti N, Rotondo JC, Cerritelli L, et al. High Human Papillomavirus DNA loads in Inflammatory Middle Ear Diseases. Pathogens. 2020;9(3):224.
10. Carbone M, Gazdar A, Butel JS. SV40 and human mesothelioma. Transl Lung Cancer Res. 2020;9(S1):S47-S59.
11. Hirose S, Takayama N, Nakamura S, et al. Immortalization of erythroblasts by c-MYC and BCL-XL enables large-scale erythrocyte production from human pluripotent stem cells. Stem Cell Rep. 2013;1(6):499-508.
12. Lee E, Lim ZR, Chen HY, et al. Defined Serum-Free Medium for Bioreactor Culture of an Immortalized Human Erythroblast Cell Line. Biotechnol J. 2018;13(4):e1700567.
13. Kurita R, Suda N, Sudo K, et al. Establishment of immortalized human erythroid progenitor cell lines able to produce enucleated red blood cells. PLoS One. 2013;8(3):e59890.
14. Olivier E, Qiu C, Bouhassira EE. Novel, High-Yield Red Blood Cell Production Methods from CD34-Positive Cells Derived from Human Embryonic Stem, Yolk Sac, Fetal Liver, Cord Blood, and Peripheral Blood. Stem Cells Transl Med. 2012;1(8):604-614.
15. Ferguson DCJ, MacInnes KA, Daniels DE, Frayne J. Chapter 1 - iPSC-derived erythroid cells. In: Birbrair A, ed. Recent Advances in iPSC-Derived Cell Types: Academic Press. 2021 pp.1-30.
16. Qiu C, Olivier EN, Velho M, Bouhassira EE. Globin switches in yolk sac-like primitive and fetal-like definitive red blood cells produced from human embryonic stem cells. Blood. 2008;111(4):2400-2408.
17. Olivier EN, Zhang SP, Yan Z, et al. PSC-RED and MNC-RED: Albumin-free and low-transferrin robust erythroid differentiation protocols to produce human enucleated red blood cells. Exp Hematol. 2019;75:31-52.
18. Griffiths RE, Kupzig S, Cogan N, et al. Maturing reticulocytes internalize plasma membrane in glycophorin A–containing vesicles that fuse with autophagosomes before exocytosis. Blood. 2012;119(26):6296-6306.
19. Bayley R, Ahmed F, Glen K, Mccall M, Stacey A, Thomas R. The productivity limit of manufacturing blood cell therapy in scalable stirred bioreactors. J Tissue Eng Regen Med. 2018;12(1):e368-e378.
20. Sivalingam J, Su EY, Lim ZR, et al. A Scalable Suspension Platform for Generating High-Density Cultures of Universal Red Blood Cells from Human Induced Pluripotent Stem Cells. Stem Cell Reports. 2021;16(1):182-197.
21. Kweon S, Kim S, Baek EJ. Current status of red blood cell manufacturing in 3D culture and bioreactors. Blood Res. 2023;58(S1):S46-S51.
22. Worobec AS, Semere T, Nagata H, Metcalfe DD. Clinical correlates of the presence of the asp816Val c-kit mutation in the peripheral blood mononuclear cells of patients with mastocytosis. Cancer. 1998;83(10):2120-2129.
23. James C, Ugo V, Le Couédic J-P, et al. A unique clonal JAK2 mutation leading to constitutive signalling causes polycythaemia vera. Nature. 2005;434(7037):1144-1148.
24. Couch T, Murphy Z, Getman M, Kurita R, Nakamura Y, Steiner LA. Human erythroblasts with c-Kit activating mutations have reduced cell culture costs and remain capable of terminal maturation. Exp Hematol. 2019;74:19-24.

25. Wu H, Klingmüller U, Besmer P, Lodish HF. Interaction of the erythropoietin and stem-cell-factor receptors. Nature. 1995;377(6546):242-246.
26. Van Gassen S, Callebaut B, Van Helden MJ, et al. FlowSOM: Using self-organizing maps for visualization and interpretation of cytometry data. Cytometry A. 2015;87(7):636-645.
27. Stolarek I, Samelak-Czajka A, Figlerowicz M, Jackowiak P. Dimensionality reduction by UMAP for visualizing and aiding in classification of imaging flow cytometry data. iScience. 2022;25(10):105142.
28. Talevich E, Shain AH, Botton T, Bastian BC. CNVkit: Genome-Wide Copy Number Detection and Visualization from Targeted DNA Sequencing. PLOS Computational Biology. 2016;12(4):e1004873.
29. Quintelier K, Couckuyt A, Emmaneel A, Aerts J, Saeys Y, Van Gassen S. Analyzing high-dimensional cytometry data using FlowSOM. Nat Protoc. 2021;16(8):3775-3801.
30. Mcinnes L, Healy J, Saul N, Großberger L. UMAP: Uniform Manifold Approximation and Projection. J Open Souce Softw. 2018;3(29):861.
31. Akin C, Arock M, Valent P. Tyrosine kinase inhibitors for the treatment of indolent systemic mastocytosis: Are we there yet? J Allergy Clin Immunol. 2022;149(6):1912-1918.
32. Wessely O, Deiner EM, Beug H, Von Lindern M. The glucocorticoid receptor is a key regulator of the decision between self-renewal and differentiation in erythroid progenitors. EMBO J. 1997;16(2):267-280.
33. England SJ, McGrath KE, Frame JM, Palis J. Immature erythroblasts with extensive ex vivo self-renewal capacity emerge from the early mammalian fetus. Blood. 2011;117(9):2708-2717.
34. Lacombe C, Mayeux P. Biology of erythropoietin. Haematologica. 1998;83(8):724-732.
35. Bai J, Fan F, Gao C, et al. CD169-CD43 interaction is involved in erythroblastic island formation and erythroid differentiation. Haematologica. 2023;108(8):2205-2217.
36. Storry JR, Olsson ML, Reid ME. Application of DNA analysis to the quality assurance of reagent red blood cells. Transfusion. 2007;47(s1):73S-78S.
37. Ching E. Solid Phase Red Cell Adherence Assay: a tubeless method for pretransfusion testing and other applications in transfusion science. Transfus Apher Sci. 2012;46(3):287-291.
38. Zingariello M, Bardelli C, Sancillo L, et al. Dexamethasone Predisposes Human Erythroblasts Toward Impaired Lipid Metabolism and Renders Their ex vivo Expansion Highly Dependent on Plasma Lipoproteins. Front Physiol. 2019;10:281.
39. Ashley RJ, Yan H, Wang N, et al. Steroid resistance in Diamond Blackfan anemia associates with p57Kip2 dysregulation in erythroid progenitors. J Clin Invest. 2020;130(4):2097-2110.
40. Flygare J, Rayon Estrada V, Shin C, Gupta S, Lodish HF. HIF1alpha synergizes with glucocorticoids to promote BFU-E progenitor self-renewal. Blood. 2011;117(12):3435-3444.
41. Hwang Y, Futran M, Hidalgo D, et al. Global increase in replication fork speed during a p57(KIP2)-regulated erythroid cell fate switch. Sci Adv. 2017;3(5):e1700298.
42. Ahmad F, Murata T, Shimizu K, Degerman E, Maurice D, Manganiello V. Cyclic Nucleotide Phosphodiesterases: important signaling modulators and therapeutic targets. Oral Dis. 2015;21(1):e25-e50.
43. Olivier EN, Marenah L, McCahill A, Condie A, Cowan S, Mountford JC. High-Efficiency Serum-Free Feeder-Free Erythroid Differentiation of Human Pluripotent Stem Cells Using Small Molecules. Stem Cells Transl Med. 2016;5(10):1394-1405.
44. Diaz MF, Li N, Lee HJ, et al. Biomechanical forces promote blood development through prostaglandin E2 and the cAMP-PKA signaling axis. J Exp Med. 2015;212(5):665-680.
45. Boer AK, Drayer AL, Vellenga E. cAMP/PKA-mediated regulation of erythropoiesis. Leuk Lymphoma. 2003;44(11):1893-1901.
46. Belegu M, Beckman B, Fisher JW. beta-Adrenergic blockade of prostaglandin E2- and D2-induced erythroid colony formation. Am J Physiol. 1983;245(5 Pt 1):C322-327.
47. Fisher JW, Radtke HW, Jubiz W, Nelson PK, Burdowski A. Prostaglandins activation of erythropoietin production and erythroid progenitor cells. Exp Hematol. 1980;8(Suppl 8):65-89.
48. Francis RO. Chapter 42 - Irradiation of Blood Products. In: Shaz BH, Hillyer CD, Reyes Gil M, eds. Transfusion Medicine and Hemostasis (Third Edition): Elsevier. 2019 pp.261-265.
49. Shi J, Yuan B, Hu W, Lodish H. JAK2 V617F stimulates proliferation of erythropoietin-dependent erythroid progenitors and delays their differentiation by activating Stat1 and other nonerythroid signaling pathways. Exp Hematol. 2016;44(11):1044-1058.

50. Nilsri N, Jangprasert P, Pawinwongchai J, Israsena N, Rojnuckarin P. Distinct effects of V617F and exon12-mutated JAK2 expressions on erythropoiesis in a human induced pluripotent stem cell (iPSC)-based model. Sci Rep. 2021;11(1):5255.
51. Kim R, Ah, Olsen L, Jayme, England J, Samantha, et al. Bmi-1 Regulates Extensive Erythroid Self-Renewal. Stem Cell Rep. 2015;4(6):995-1003.
52. Liu S, Wu M, Lancelot M, et al. BMI1 enables extensive expansion of functional erythroblasts from human peripheral blood mononuclear cells. Mol Ther. 2021;29(5):1918-1932.
53. Stutchfield CJ, Jain A, Odd D, Williams C, Markham R. Foetal haemoglobin, blood transfusion, and retinopathy of prematurity in very preterm infants: a pilot prospective cohort study. Eye. 2017;31(10):1451-1455.

**Figure legends:**

**Figure 1: Differentiation of KitD816V iPSCs**

A: Diagram and table illustrating the long chemically-defined PSC-RED protocol to differentiate iPSCs into erythroid cells. STIF: S =SCF; T = Tpo; I = IGF-2; F = bFGF. SEDI: S = SCF; E = Epo; D = Dex; I = IBMX. SER and SER2: S = SCF; E = Epo; R = RU486. Concentrations of all components are provided in the online method section. The short version of the protocol is similar except that the expansion in STIF between day 10 and 17 is omitted. The short version yields RBCs that express more embryonic globin than the long protocol.

B: Growth curve of iPSCs hemizygous (line A4) or homozygous (line B34) for the D816V mutation. The control O1 cells were differentiated according to the PSC-RED protocol including SCF. The A4 and B34 lines were differentiated according to the same protocol but SCF was omitted at all steps.

C: A 15-color flow cytometry assay was used to examine the antigen expression profiles of differentiating cells that we collected weekly between day 10 and 45. Dimensionality reduction analysis using flowSOM and U-MAP revealed that dividing the cells into 8 major populations according to expression of 10 markers provided a useful summary of the evolution of the cells undergoing the PSC-RED protocol. Heatmap summarizes the relative expression of the 10 markers used to define the 8 populations. Populations expressing CD34 were labelled HPC1 to 4 while populations negative for this marker but positive for erythroid markers were labelled Ery1 to 4.

D. UMAP analysis. Data from the 15-color Flow cytometry analysis of control A4 and B34 cells assessed weekly from day 10 to 45 was concatenated and analyzed using UMAP generating the pattern illustrated in D. The concatenated data was then analyzed with flowSOM which segmented the data into 12 populations. Four populations representing each less than 1% of the cells and were eliminated. The UMAP graph was then colors with the 8 remaining major populations which represented more than 96% of all cells.

E. Chart summarizes the evolution of the 8 populations defined by FlowSOM during erythroid differentiation. At day 10, the phenotype of the A4 and B34 cells is similar to the control cells with populations of 43+;34+;45- HPC1 and HPC2 (which differed by expression of CD235a) dominating the culture. At days 17 and 24, the control cells differentiated progressively into populations of 45+ HPC4 and 45+ Ery1 cells. At day 31, Ery2 cells (34low; 45+; 36low; 71+; 235a+) resembling pro-Erythroblasts and Ery3 cells (34-; 45- ; 36+; 71+; 235a+) resembling basophilic erythroblasts became prominent and matured into Ery4 late erythrocytes (34-; 45-; 36-; 71low; 235a+) by day 38. In the kit mutated clones, the HPC2 and Ery1 cells did not amplify to the same degree as in the control cells,

and the Ery2 cells were barely detectable. Instead, an HPC3 population with a phenotype intermediate between HPC1 and 2 briefly expanded and, most notably, the Ery3 population became prominent much earlier, particularly in the homozygous B4 cells. The Ery3 cells from the A4 cells eventually differentiated into Ery4 cells, but those from the B34 clone did not, resulting, at days 31 and 38, in cultures composed almost exclusively of Ery3 cells. Because of massive cell death of the B34 cells during the last week of differentiation, a FACS analysis was not performed at day 45 for these cells.

**Figure 2: Differentiation in the absence of SCF and Epo.**

A: Diagram illustrating the differentiation conditions. The * indicates the absence of SCF in supplement S2 and S3. See figure 1A for details.

B: Growth curves illustrating the proliferation of the A4 and B34 in the absence of SCF and Epo. Results of one experiments representative of two experiments are shown.

Both hemizygous and homozygous D816V lines can differentiate in the absence of both SCF and Epo. In the absence of SCF and Epo, B34 Ery3 cells did not die as quickly upon withdrawal of Dex when Epo was absent from the culture media, and some of the cells were even able to complete their terminal differentiation and enucleate at a rate of about 5%. This suggests that the block of differentiation of the Ery3 cells in the B34 cells is likely due to overstimulation by the homozygous kitD816V, and that this overstimulation can be partly relieved by omitting Epo from the media.

C: Diagram illustrating the 15-color FACS analysis of differentiation in the absence of SCF and Epo.

**Figure 3: Terminal differentiation of KitD816V iPSCs**

A: Representative dotplots illustrating the enucleation of the A4 cells differentiated in the absence of SCF, with or without 200nM dasatinib (introduced on day 31 of differentiation). Experiment was performed in duplicate.

B: Micrograph illustrating the morphology of the cells obtained on day 45 of the PSC-RED protocol. Inset: cell pellet obtained on day 45 is highly hemoglobinized.

C: Graph illustrating the evolution of the cultures between day 31 to day 45 in the presence or absence of dasatinib. Cells were classified using morphological criteria after Romanowsky staining and light microscopy examination.  Baso = basophilic Erythroblasts; Poly = poly-chromatophilic erythroblasts; Ortho = ortho-chromatophilic erythroblasts; retic = reticulocytes. Dasatinib accelerates the

differentiation and increases the rate of enucleation. One hundred cells were enumerated at each time point.

D: HPLC profiles of erythroblasts obtained from clone A4 (in the absence of SCF)

E: Bargraph illustrating the averages (± S.D.) globin chain expression measured in three experiments. RBCs produced by clone A4 express mostly fetal hemoglobins.

**Figure 4: Production of self-renewing erythroblasts**

A: Diagram illustrating the differentiation conditions. The * indicates the absence of SCF in supplement S2 and S3. See Figure 1A for details.

B: Growth curves illustrating that day-17 HPCs derived from the A4 and B34 cells can differentiate into erythroblasts that can self-renew for about 45 to 55 days in the presence of Dex and IBMX but in the absence of any cytokines, yield a more than 1,000-fold amplification. Averages (± S.D.) of two experiments are shown.

C: Growth curve illustrating that day-17 HPCs derived from the A4 cells can differentiate into erythroblasts that can self-renew for > 140 days in the presence of Dex and IBMX and 1u/mL of erythropoietin, yielding more than a $10^{20}$-fold amplification. Averages (± S.D.) of two experiments are shown.

D: Growth curves illustrating the differentiation of 4 lines of iPSCs hemizygous for the KitD816V mutation and either hemizygous (H5 and H11) or homozygous for the Jak2V617F mutations. All four iPSC lines proliferate and differentiate in the absence of SCF and Epo at rate that are greater than that of control cells (O1) differentiated in the presence of SCF and Epo. Averages (± S.D.) of two experiments are shown.

E: Growth curves illustrating that day-17 HPCs derived from the H5/H11 and G18/H12 iPSC lines can differentiate into erythroblasts that can respectively self-renew for about 120 and 100 days in the presence of Dex and IBMX but in the absence of any cytokines, yielding > $10^{18}$-fold amplification in the case of the H5 and H11 lines and > $10^{16}$-fold amplification for the G19 and H12 lines. Average (± S.D.) of two SREs are shown for each genotypes.

F: Bargraph illustrating the expression of 11 markers in the A4 kitD816V SRE (cultured in EDI condition) and in the kitjak2 line H5 and H11 (cultured in DI conditions). Bars represent the average (± S.D.) expression measured in two independent experiments for the A4 kitD816V SREs and the average (± S.D.) expression of the H5 and H11 SREs measured weekly from day 17 to 93. The day-17

HPCs (black bars) differentiate into SREs between days 17 and 31. After day 31, expression of the markers is very stable over time. SREs resemble iPSC-derived late CFU-E or pro-Erythroblasts.

**Figure 5: Differentiation of the self-renewing erythroblasts**

A: Differentiation conditions.

B: Growth curve illustrating the average cell growth and viability ± S.D. (n=3) during H5 SREs differentiation.

C: Dotplots illustrating the expression of CD235a, CD43, CD36 and CD71 during H5 kitJak2 SREs differentiation. Expression of CD235a increases overtime, while CD43, CD36 and CD71 are sequentially silenced. Uns. = unstained

D: Micrographs illustrating a Romanovsky stain of cells generated from the H5 SREs after 10 days of differentiation. Most cells are reticulocytes or orthochromatic erythroblasts. Inset: cell pellet obtained at day 9 illustrates the strong hemoglobinization of the cells.

E: Differentiating H5 SREs were analyzed by FACS after staining with DAPI and annexin V-FITC. bar graph illustrates the average percentage ± S.D. (n=3) of necrotic, late and early apoptotic cells at days 3, 6, 9 and 11.

F: left: dotplots illustrating a flow cytometry analysis of H5 cells stained with Draq5 at day 10 of differentiation. Right: the three bar graphs respectively illustrate the percentage enucleation, the cumulated fold-amplification at day 10 or 11 (calculated as the product of the fold-amplification observed after each feeding between days 0 and 10 or 11), and the number of cRetic /SREs (calculated by multiplying the rate of enucleation by the cumulated fold-amplification at day 10 or 11). The averages (± S.D.) of 5 experiments are plotted.

G: right: chromatogram illustrating a reverse phase HPLC analysis of globin chain expression of cRetics obtained by differentiation of A4 and H5 self-renewing erythroblasts. Bargraphs illustrate the averages (± S.D.) of two experiments.

E: left: red cell indices of cells generated from the A4 and H5 lines obtained using an Advia blood count analyzer. (n=3); CHCM = cellular hemoglobin concentration mean of intact RBCs (optically measured MCHC); CH = mean optical hemoglobin content of intact RBCs. right: red cell diameter assessed by microscopy. 100 cells /cell type were analyzed.

**Figure 6: Copy-number analysis by low-pass sequencing**

Genomic DNA was sequenced at a depth of 1.5Gb and analyzed using the CNVkit software. Graphs illustrate that PB MNC O1, and passage 20 to 25 A4, H5, H11, G19 and H12 SREs exhibit no

detectable copy number variants greater than 1mb (the limit of detection for this read depth). By contrast, transformed cells, HUDEP-2 and K562 cells, cultured for a long period of time exhibit a high level of aneuploidy.

**Figure 7: cRBC as reagent RBCs in a solid-phase red cell adherence assay**

Treated-capture strips were coated as suggested by the manufacturer (Immucor) with about 5 million A4 cultured RBCs or with control adult RBCs of known (NYBC samples) RhCcE phenotypes. The phenotypes of the coated cells were then determined by solid phase red cell adherence assay using test antibodies and IgG-coated indicator RBCs also as recommended by the manufacturer. In this system, a visible red pellet at the bottom of the well indicates absence of the antigen on the tested RBCs, while the absence of a pellet indicates presence of the antigen. The phenotypes determined with this capture assay agreed in all cases with the expected (known) phenotypes, demonstrating that cRBCs can be used as reagent RBCs in this system. NYBC1 to 3 are control adults RBC samples.

# Figure 1

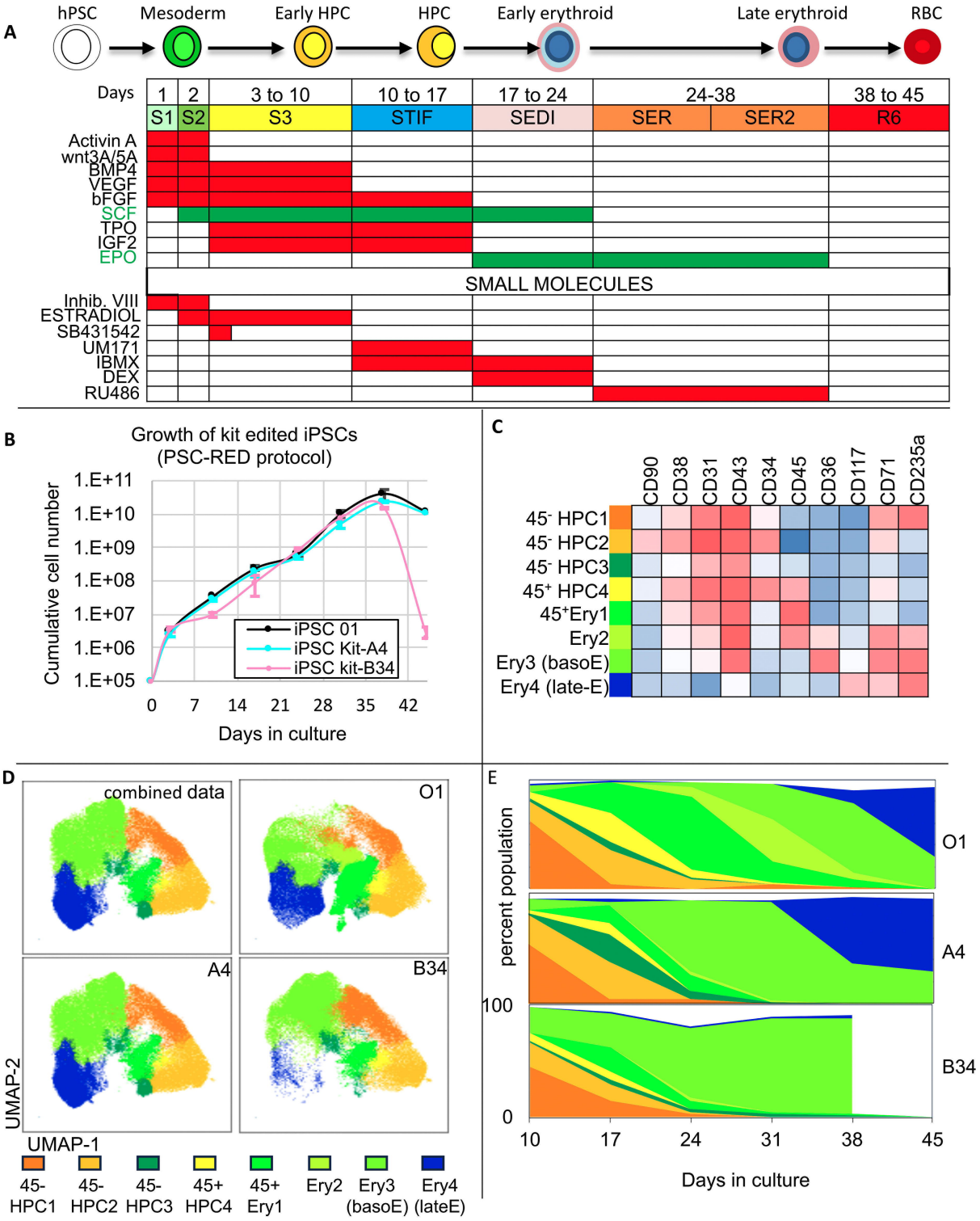
A
hPSC
Mesoderm
Early HPC
HPC
Early erythroid
Late erythroid
RBC
Days
1
2
3 to 10
10 to 17
17 to 24
24-38
38 to 45
S1
S2
S3
STIF
SEDI
SER
SER2
R6
Activin A
wnt3A/5A
BMP4
VEGF
bFGF
SCF
TPO
IGF2
EPO
SMALL MOLECULES
Inhib. VIII
ESTRADIOL
SB431542
UM171
IBMX
DEX
RU486
B
Growth of kit edited iPSCs
(PSC-RED protocol)
Cumulative cell number
1.E+11
1.E+10
1.E+09
1.E+08
1.E+07
1.E+06
1.E+05
0
7
14
21
28
35
42
Days in culture
iPSC 01
iPSC Kit-A4
iPSC kit-B34
C
CD90
CD38
CD31
CD43
CD34
CD45
CD36
CD117
CD71
CD235a
45- HPC1
45- HPC2
45- HPC3
45+ HPC4
45+Ery1
Ery2
Ery3 (basoE)
Ery4 (late-E)
D
combined data
O1
A4
B34
UMAP-2
UMAP-1
45- HPC1
45- HPC2
45- HPC3
45+ HPC4
45+ Ery1
Ery2
Ery3 (basoE)
Ery4 (lateE)
E
percent population
100
0
O1
A4
B34
10
17
24
31
38
45
Days in culture

# Figure 2

A

| cells | cytokines | 1 | 2 | 3 to 10 | 10 to 17 | 17 to 24 | 24-31 | 24-38 | 38 to 45 |
|---|---|---|---|---|---|---|---|---|---|
| O1 | Epo + SCF | S1 | S2 | S3 | STIF | SEDI | SER | SER2 | |
| A4 & B34 | Epo | S1 | S2* | S3* | TIF | EDI | ER | ER2 | |
| | none | | | | | DI | D | R | |

B

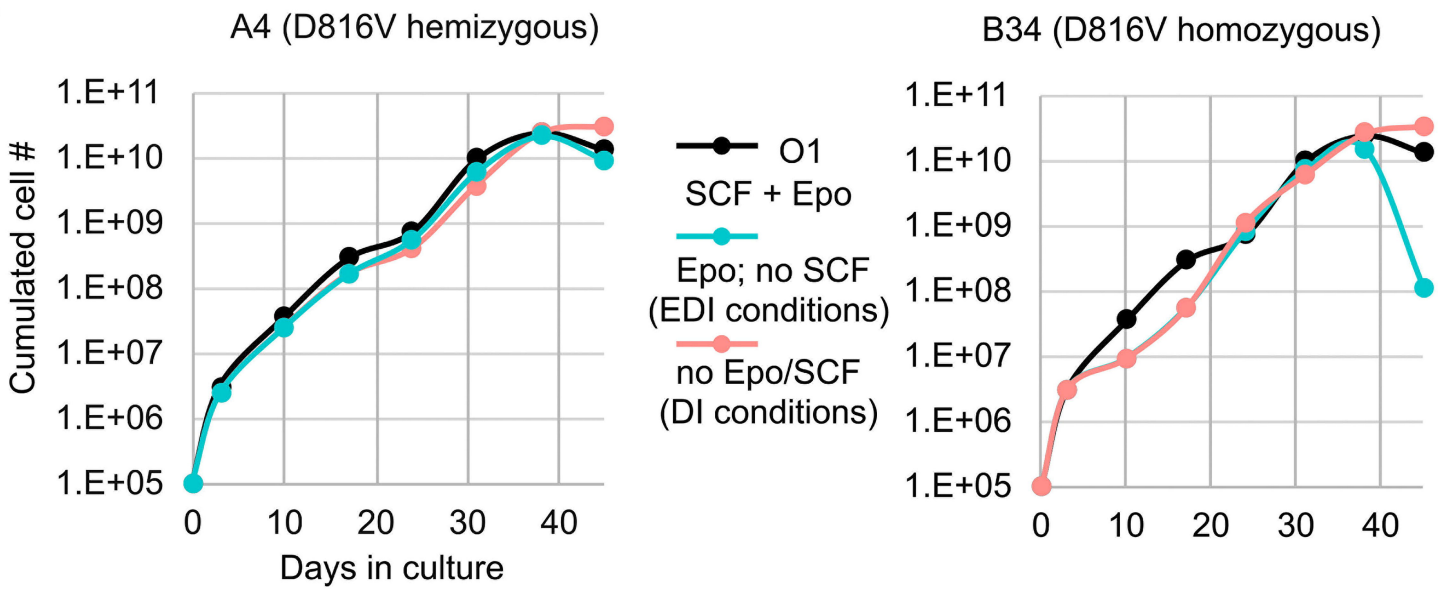


C

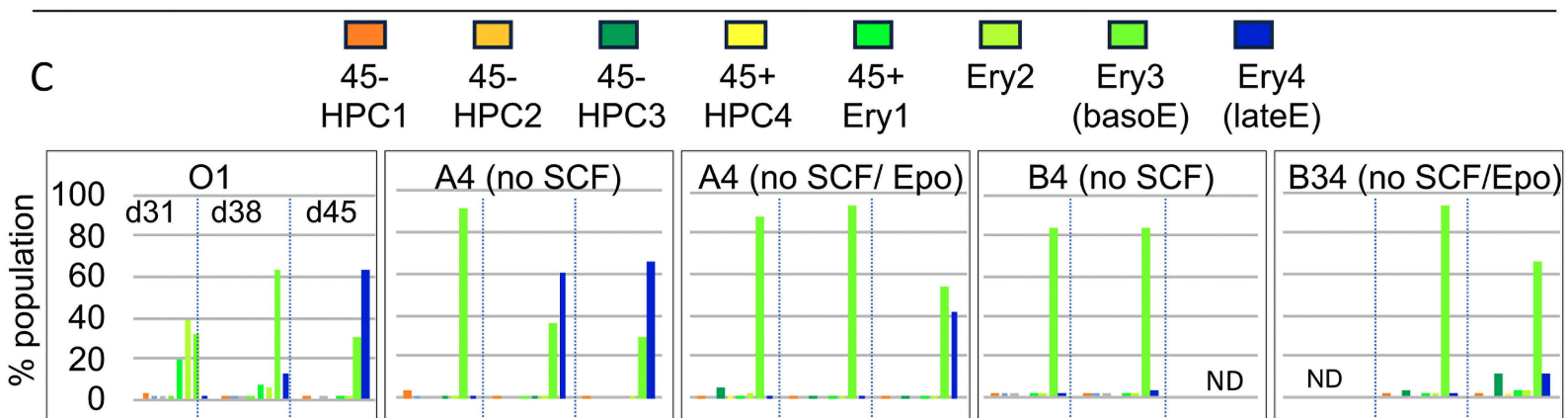

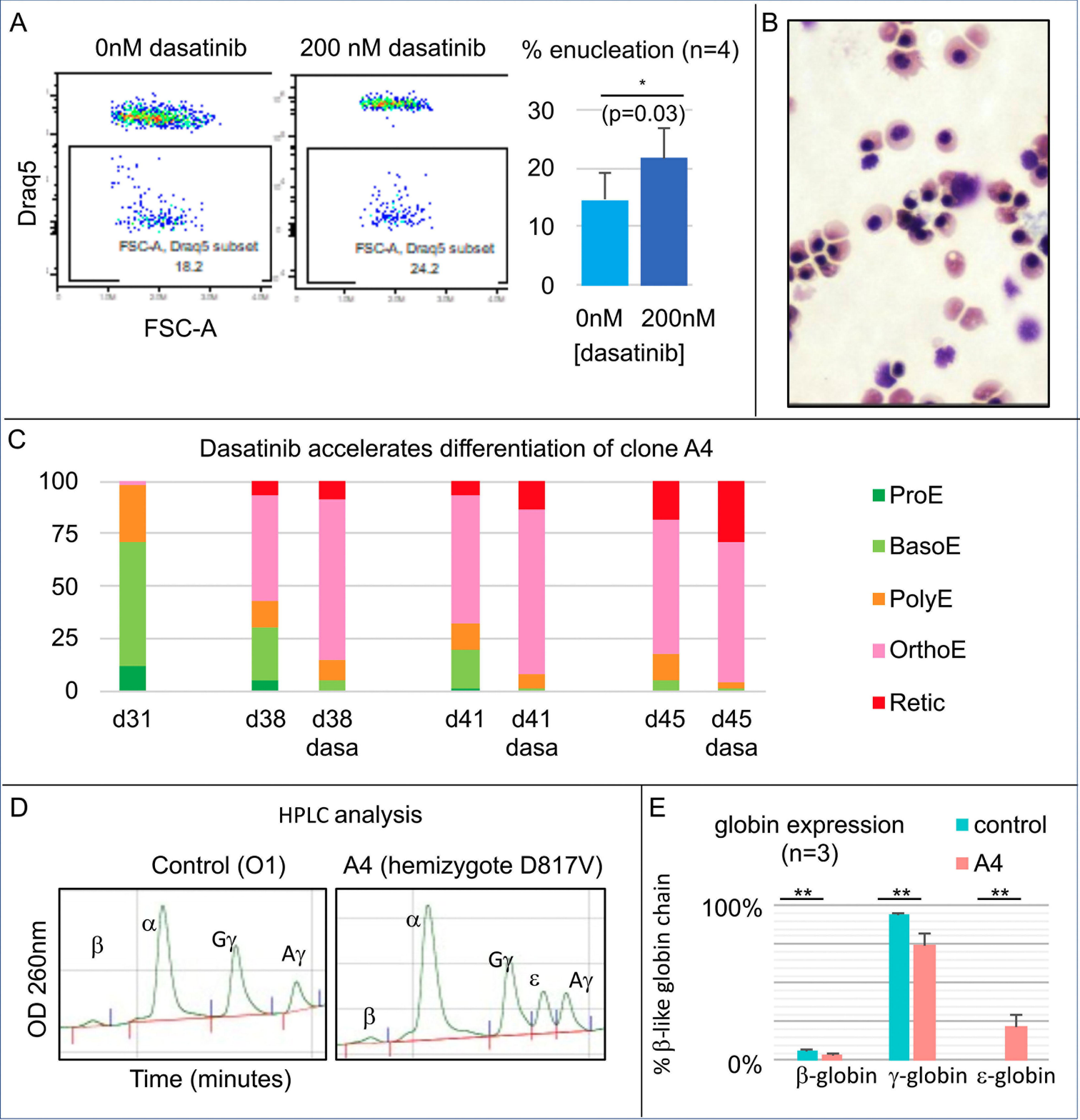
A
0nM dasatinib
200 nM dasatinib
% enucleation (n=4)
Draq5
FSC-A, Draq5 subset
18.2
FSC-A, Draq5 subset
24.2
FSC-A
*
(p=0.03)
30
20
10
0
0nM
200nM
[dasatinib]
B
C
Dasatinib accelerates differentiation of clone A4
100
75
50
25
0
d31
d38
d38 dasa
d41
d41 dasa
d45
d45 dasa
ProE
BasoE
PolyE
OrthoE
Retic
D
HPLC analysis
Control (O1)
A4 (hemizygote D817V)
OD 260nm
β
α
Gγ
Aγ
ε
Time (minutes)
E
globin expression (n=3)
control
A4
% β-like globin chain
100%
0%
**
β-globin
γ-globin
ε-globin

A

| days | protocol | 1 | 2 | 3-10 | 10-17 | 17-24 | 24-31 | 31-38 | 38 - indefinite |
|---|---|---|---|---|---|---|---|---|---|
| control | PSC-RED | S1 | S2 | S3 | STIF | SEDI | SER | SER2 | |
| No SCF | | S1 | S2* | S3* | TIF | EDI | ER | ER2 | |
| No SCF/ EPO | | S1 | S2* | S3* | TIF | DI | R | R2 | |
| | | | | | | | | | |
| No SCF | Self-renewal | S1 | S2* | S3* | TIF | EDI | | | |
| No SCF/Epo | | S1 | S2* | S3* | TIF | DI | | | |

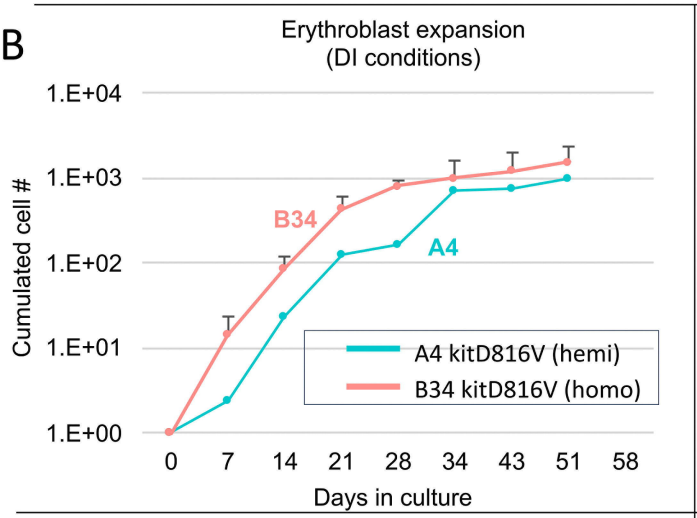


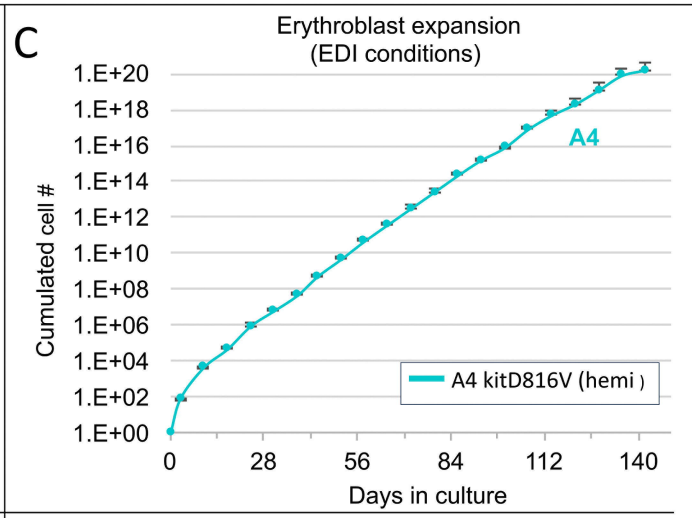


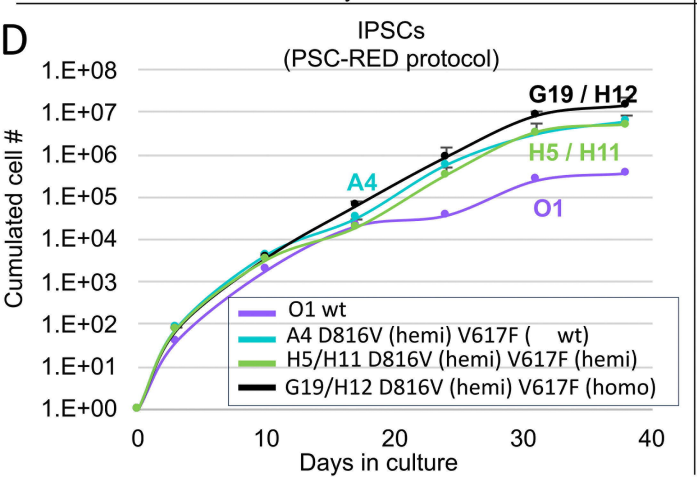


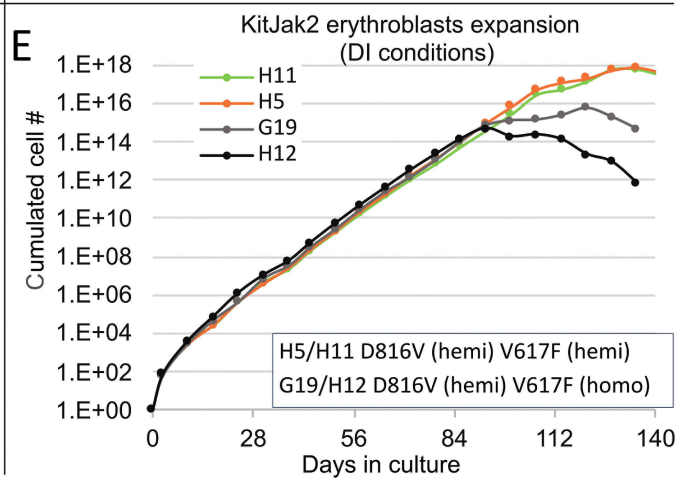


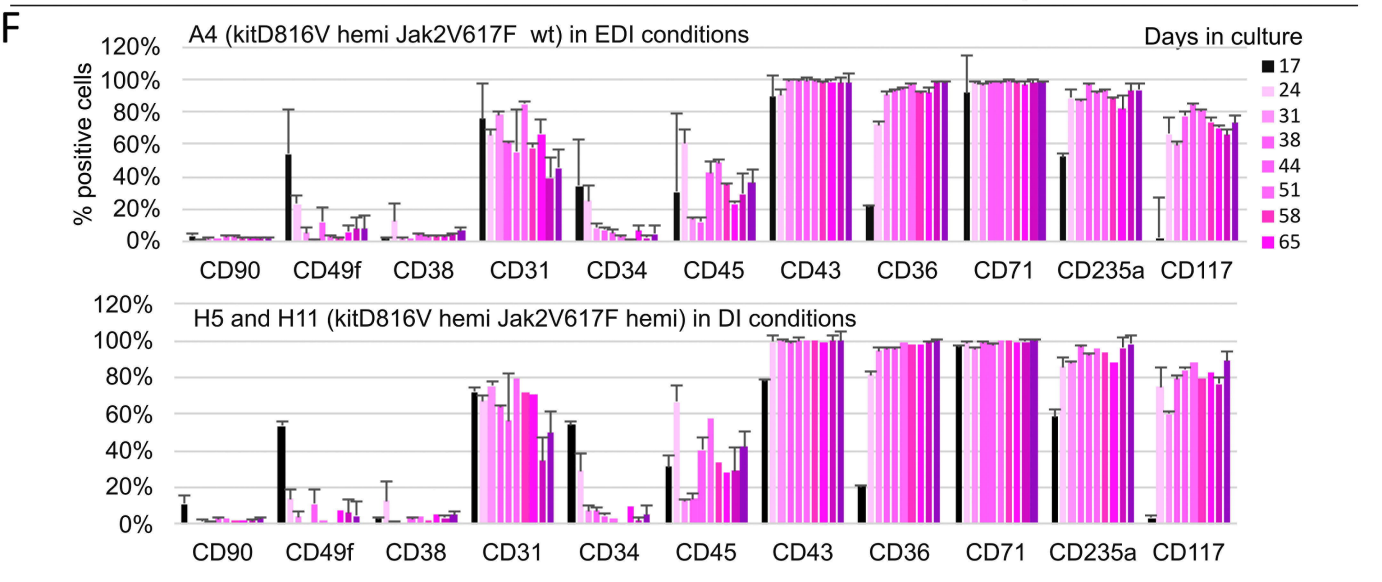


Figure 4

# Figure 5

A

| Cells | Self-renewing conditions | Day 0 - 5 | Day 5 – 11 |
|---|---|---|---|
| KitD816V (A4) | Dex Epo, IBMX | R5 medium<br>Epo 4U/mL (day 0)<br>RU486,<br>5% human plasma | Pure RPMI |
| Kit<br>(H5/H11, G19/H12) | Dex IBMX | | |

B

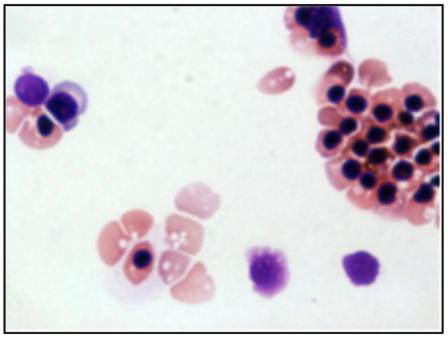

C

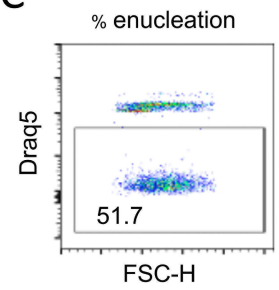


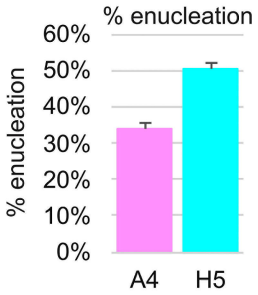


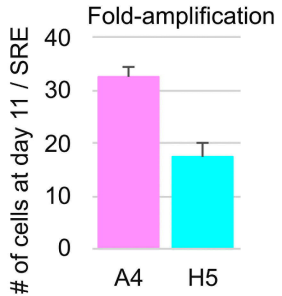


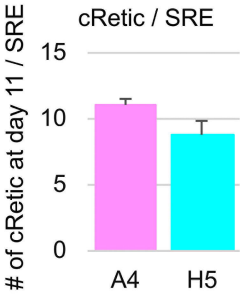


D

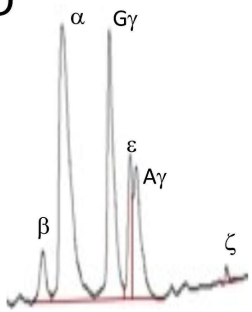


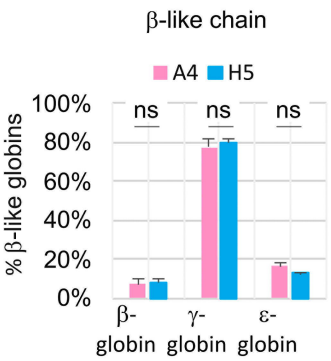


E

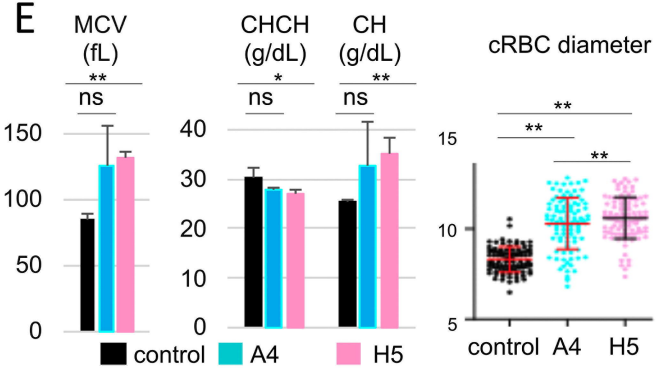

# Figure 6

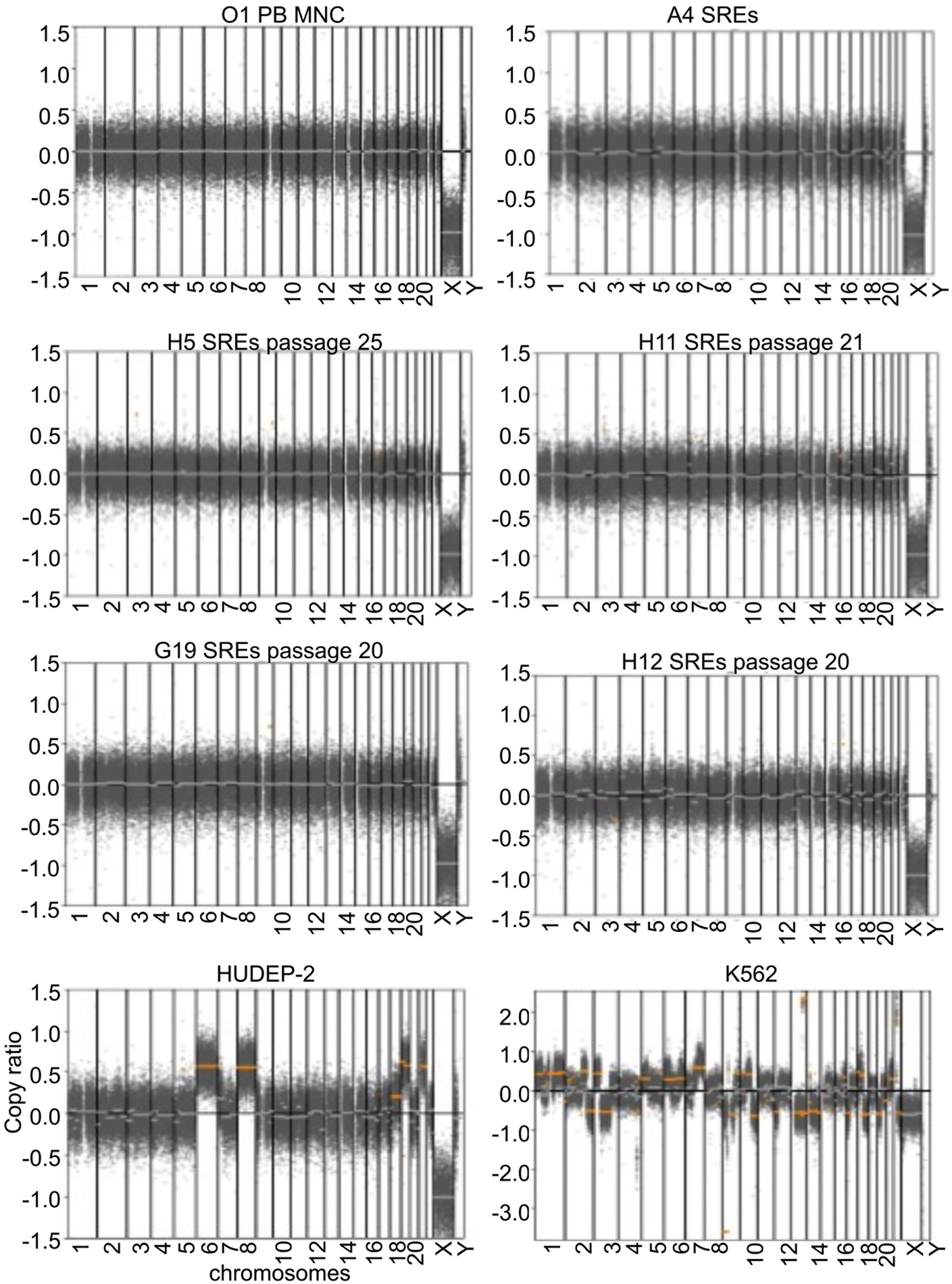
O1 PB MNC
A4 SREs
H5 SREs passage 25
H11 SREs passage 21
G19 SREs passage 20
H12 SREs passage 20
HUDEP-2
K562
Copy ratio
chromosomes

# Figure 7

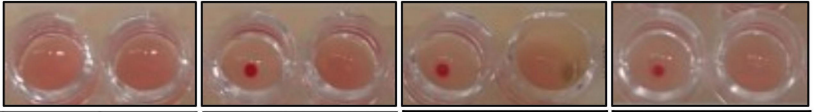

| | NYBC1 | NYBC2 | NYBC3 | | A4 reticulocytes | | A4 reticulocytes | |
|---|---|---|---|---|---|---|---|---|
| **Phenotype** | Ce | cE | ce | ce | ce | ce | c e | c e |
| **Test Ab** | e | E | C | c | E | e | C | c |
| **Result** | pos | pos | neg | pos | neg | pos | neg | pos |

**Supplementary methods:**

**Culture conditions:** All cultures were performed at 37C, in 7% $CO_2$ and in 5% oxygen.

**Pluripotent stem cell culture:** hiPSCs were maintained undifferentiated in chemically-defined conditions essentially as described by Chen et al. using E8 medium (1). Cells were grown on Vitronectin (life technologies) and passaged using EDTA every 3-4 days depending on their confluence stage.

**Differentiation of iPSCs into erythroid cells using the PSC-RED protocol:** Composition of the IMIT and R6 media and of all supplements are provided in **Tables S1 and S2**.

**On day -1**: Three-day-old iPSC colonies were dissociated with 5mM EDTA to generate small clumps that yield colonies of about 50 cells on day 0. Clumps were plated at 1–2 × $10^5$ cells/well in 2mL/well of E8 medium on vitronectin-coated six-well plates and allowed to attach overnight.

**On day 0**: Differentiation was induced by replacing the E8 medium with IMIT medium containing **supplement 1**.

**On day 2,** 6x concentrated **supplement 2** was added.

**On day 3,** the cells were dissociated with Tryple-Select, centrifuged, and plated in IMIT medium containing **supplement 3** at 1x$10^5$ cells/mL in a 6-well plate (3mL/well).

**On day 6**, the cells were centrifuged and plated at 5.$10^5$/mL in IMIT medium containing supplement 3 excluding SB431542 but including 30nM of UM171 (or with UM729 at 500 nM). An additional dose of supplement 3 (provided from a 6x concentrated stock) was added on day 8.

**On day 10,** the cells were centrifuged and re-suspended at 0.66 × $10^5$ cells/mL in IMIT medium containing the STIF supplement.

**On day 17,** the cells were centrifuged and plated at 2 × $10^5$ cells/ mL in IMIT plus GM-CSF and the SED supplement.

Note: cells obtained on day 17 (i.e., day-17 HPCs) from kit or kitjak2 mutant lines give rise to self-renewing erythroblasts when cultured as described in the self-renewing erythroblasts section.

**On day 24**, the cells were centrifuged and plated at 2 × $10^5$ cells/mL in IMIT containing the SER supplement. RU486, a Dex antagonist, is included in the SER supplement to block residual traces of Dex

**On day 31,** the cells were centrifuged and plated in R5 medium containing the SER2 supplement.

**On day 38,** the cells were centrifuged diluted to $0.5x10^6$/mL and maintained in pure R6 medium for up to 8 days.

Cells cultured between days 6 to 38 were diluted to $0.5x10^6$/mL in the appropriate media and supplement whenever their concentrations reach more than about $1.5x10^6$cells/mL. Cytokine concentrations between days 6 and 38 were refreshed by addition of 6x concentrate of the appropriate supplement every other day. 6x concentrates of each supplements were made by multiplying by 6 the concentrations of cytokines and small molecules indicated in Table S2. Concentrated supplements were used to keep the concentration of cytokine and small molecules high enough at all times without having to spin the cells and without overly increasing the cell culture volume.

1x and 6x concentrates of supplements 1, 2, 3, 4, STIF, SED and SER were prepared in IMIT. SER2 supplement was prepared in R6. All centrifugations were performed at 250g for 5 to 10 minutes (depending on volume). All culture vessels used were tissue culture-treated. Experiments were generally performed in 6-well plates, but flasks were used to obtain larger volumes.

**HPLC analysis:** Cells were washed twice with PBS and lysed in water by 3 rapid freeze-thaw cycles in dry-ice and in a 37C water bath. Debris was eliminated by centrifugation at 16 000g and the lysates stored at -80°C. HPLC were performed as described by Fabry et al. (2) Briefly, a few mL of lysate containing about 50 μg of protein in about 100 μL of 40% acetonitrile and 0.18% TFA was filtered and loaded on a VYDAC C4 column. The globins were then eluted with increasing concentration of acetonitrile during a period of about 80 minutes. The starting elution buffer was programmed to be 80% buffer A and 20% buffer B and to rise to 50% buffer B in 50 minutes. Buffer A = 36% acetonitrile and 0.18% TFA and buffer B = 56% acetonitrile and 0.18% TFA. Globin chain elution was monitored by measuring O.D. at 220 nm.

**CRSPR editing:** A nucleic acid solution containing 1ug of capped, polyadenylated cas9 mRNA substituted with modified Uridine (CLEAN-Cap cas9 mRNA, cat # L-7206 from Trilink Biotechnologies) were mixed with 4 ug of synthetic sgRNA (Sigma technologies) and 4μg of a 200-mer oligonucleotides HDR donor in 15 ml of H20. About 150,000 iPSCs dissociated with Accutase were resuspended in 15 ml of buffer P (100mM phosphate buffer pH 7.4; 15mM $NaHCO_3$; 2 mM glucose, 12mM $MgCl_2$) and mixed with 15 ml of the nucleic acid solution in a 1 cm 1/16 of an inch inner diameter electroporation chamber made of platinum-cured silicone tubing. The tube was then subjected to two 10 msec pulses of 115V using a NEPA21 (Nepagene) electroporator hooked up to Cell-Porator Voltage Booster (Life technology) resulting in a 600V pulse. Subclones were then isolated and screened for the presence of the desired mutations by amplifying and sequencing PCR fragments representing the regions of interest. In some experiments, the PCR fragments were pre-screened by digestion with an appropriate restriction enzyme. To obtain heterozygous clones, donor HDR oligonucleotides coding for

the wt sequences were mixed-in with the mutated donor HDR oligonucleotide. Sequences of the sgRNA and HDR donor DNA are provided in **Table S4**.

**Methyl-cellulose assays:** Assays were performed as suggested by the manufacturer using MethoCult™ SF H4636 (Stem Cell Technology, Vancouver, CA). For each replicate cells were tested in duplicated humidified 35mm dishes. Colonies were counted on day 14.

**Cell morphology:** Erythroid differentiation and enucleation were also assessed microscopically by Rapid Romanowsky staining (3) of cytospin preparations using the HEMA-3 kit from Fisher Scientific according to the manufacturer instructions. Cell sizes were estimated on a Nikon TE-2000S microscope using the NIS Element F software provided by the manufacturer.

**RBC filtration:** 99.5% pure populations of enucleated RBCs were generated by filtration of the cells obtained after 10 days of differentiation of self-renewing erythroblasts through PAL Acrodisc 25mm WBC filters as recommended by the manufacturer. Filtered cRetics were stored for up to one month with little signs of hemolysis in Alsever's solution (Sigma).

**Cell enumeration and viability:** Cells were counted with a Luna-FL dual channel Automated Cell Counter (Logos) using acridine orange to visualize the live cells, and propidium iodide to exclude the dead cells. Alternatively, cells were counted using a Cytek Aurora flow cytometer. Apoptosis was detected by staining with Annexin V-FITC and DAPI.

**Enucleation:** The enucleation rate was measured using the DRAQ5 DNA nuclear stain (ThermoFisher) after exclusion of dead cells with Propidium Iodide or DAPI. The cells were analyzed with a Cytek Aurora flow cytometer and the FlowJo software.

**Supplementary figure legends**

**Figure S1: Medium requirement**

A: During the PSC-RED protocol the cell number doubles on average every 48 hours, leading to > 200,000-fold amplification.

B: Graph illustrating medium consumption during the 38 days of the PSR-RED protocol to produce about $5.10^9$ RBCs (the number of RBCs present in 1 mL of blood), in low density cell culture (< $2x10^6$/mL). More than 99% of the cell culture medium is consumed after day 37 during the PSC-RED protocol. Increasing the cell culture density helps decrease the volume of culture medium, but not the amount of cytokines, because cytokines are generally internalized and are not recycled.

**Figure S2: Insertion of the D816V mutation in the kit gene using CRSPR/cas9**

Top: Three nucleotide substitutions were introduced into the donor oligonucleotide DNA. A C to G transversion which destroys the PAM was introduced to increase the overall rate of mutation by preventing re-mutation of CRSPR modified alleles after homologous recombination. Two nucleotide substitutions were also introduced to change codon 816 from GAC (ASP) to GTG (valine). Complete sequence of the donor oligonucleotide is provided in the methods section.

Middle: Chromatograms illustrating the sequences of clone B34 and A4 which were selected for further studies.

Bottom: Protein sequence of the alleles that we generated. Clone B34 is homozygous for the D816V mutation. Allele A of clone A4 carries the D816V allele. Allele B contains a 1 base insertion that leads to a frame shift at position 816 resulting in a stop codon at position 820.

**Figure S3: Romanowsky staining of IPSCs differentiated according to the PSC-RED protocol:**

iPSCs O1 (controls) were differentiated according to the PSC-RED protocol. iPSCs A4 (kitD816V hemizygous) and B34 (kitD816V homozygous) were differentiated with the same protocol but SCF was omitted at all steps. About 100,000 cells were collected at days 10, 17, 24, 31, 38 and 45, cytospined on poly-lysine treated slides, stained using the Romanowsky protocol. Cells progressively differentiate into mature erythroid cells.

**Figure S4: Flow cytometry analysis of control, A4 and B34 iPSCs during the PSC-RED protocol**

A: A 15-color flow cytometry assay was used to monitor erythroid differentiation using the PSC-RED protocol. Cells were segmented into 8 major populations according to expression of 10 markers using flowSOM. Heatmap illustrates the expression of the 10 markers used to define the 8 populations. The scatterplots illustrate the evolution of each population. The Ery3 and Ery4 populations become dominant much earlier in the A4 and B34 clones.

B: The same experiment was repeated on later passage iPSCs with new lots of antibodies. FlowSOM was used using the same parameters to segment the data into 8 cell populations. As in A, populations of erythroid cells arise earlier in the kitD816V mutated clones.

C: Dotplots illustrating expression of 11 markers during PSC-RED erythroid differentiation of iPSC O1 (grown in the presence of SCF and Epo) and of iPSC clones A4 and B34 (both grown in the absence of SCF).

**Figure S5: Methyl cellulose assays**

iPSCs O1 (controls) were differentiated according to the PSC-RED protocol. iPSCs A4 (kitD816V hemizygous) and B34 (kitD816V homozygous) were differentiated with the same protocol but SCF was omitted at all steps. Respectively, 1,500, 3,000 and 10,000 cells were collected at days 10, 17, 24 and plated in duplicate into methyl-cellulose. Colonies were counted after 14 days of incubation. Histograms summarize the results of two experiments. The total number of colonies decreases from day 10 to day 24. No significant differences in the myeloid potential between the cells derived from the O1, A4 and B34 iPSC lines was detected.

**Figure S6: D816V heterozygous clones**

A: iPSCs O1 and O2 were transfected with cas9 mRNA, an sgRNA and two oligo donors' DNA: a mutated and an unmutated oligo. MboI was used to identify 96 clones having at least one V816 allele. For both O1 And O2 about 20% of the clones were positive for the MboI restriction sites. Of those, about half were heterozygous for the D816V mutation. Top line: wild type genomic sequence; middle: donor oligonucleotide coding for a D at position 816. Bottom line: mutated donor oligonucleotide coding for a V at position 816. Bottom chromatogram illustrates the sequence of one of the heterozygous clones selected for further studies.

B. Representative growth curves illustrating the proliferation of clones heterozygous for the D816V mutation isolated from donors O1 (clone D14) and O2 (clone CP) during the PSC-RED protocol (n=2) as compared to clone A4.

C: Bargraph illustrating enucleation rate of the same clones as evaluated by staining with Draq5 (n=2).

D: Dotplots illustrating expression of 11 markers during PSC-RED erythroid differentiation of kit D816V iPSC A4, O1 and O2 in the absence of SCF.

**Figure S7: kitD816V SREs grown in DI conditions (Dex and IBMX but no cytokines).**

A: Day-17 HPCs derived from the A4 and B34 iPSCs lines were differentiated according to the PSC-RED protocol omitting SCF and placed in culture with only Dex and IBMX (DI conditions) to assess their self-renewal potential. In parallel experiments, the day-17 HPCs were differentiated into mature erythroid according to the PSC-RED protocol until day 45 (omitting SCF). Flow cytometry using a 15-color assay was performed weekly between day 17 and day 52 on the cells cultured in DI conditions. the A4 and B34 day-17 HPCs downregulated CD49f, CD45, CD38 and CD34 and upregulated expression of CD36, CD71, and CD235a (Figure S7A). This transition from an HPC to an erythroblast phenotype, resembling iPSC-derived late CFU-Es and pro-erythroblasts, was almost completed by day 24. After that time point the antigen profiles of both the A4 and B34 cells remained constant until day 45.

B: Romanowsky staining supported these findings. Day-17 HPCs grown in DI condition exhibit a CFU-E/pro-erythroblast morphology at day 45.

**Figure S8: Viability of the A4 and H5 SREs:**

A4 and H5 SREs were cultured in DI conditions for about 135 days. The blue curve illustrates the cumulated cell number. The pink curve the viability assessed by propidium iodide staining. The viability was very high, generally 98 to 99% until senescence. A dip of the viability to about 90% was observed whenever the cells were allowed to reach concentrations above $2.10^6$ cells / mL.

**Figure S9: Production and FACS analysis of the jak2V617F mutant**

A: Design of the donor oligonucleotide: Sequence of the wild-type (wt) and modified sequences.

B: Chromatograms illustrating the sequence of the region around jak2 position 657 in A4; H5 and H12 cells.

Ther A4 line has no modification at this position (homozygous 657V); H12 is homozygous for 657F and H5 is heterozygous for 657F and for a 2 amino acid deletion at position 655 and 656.

C: Dotplot illustrating expression of 11 markers during PSC-RED erythroid differentiation of iPSCs A4, G19 and H5 in the absence of SCF and Epo.

**Figure S10: Flow cytometry analysis of the SREs**

A: Dotplots illustrate the expression of 11 markers of A4 D816V erythroblasts that had been in culture for 93 days. CD90, 49f, 38 and 34 are barely expressed; CD31 and 45 are expressed at low levels; CD43, 36, 71 and 235a are expressed at high levels in almost all cells. CD117 (the SCF receptor) is expressed at a high level but only in about two-thirds of the cells.

B: left: Bargraph illustrating the expression of 11 markers in kitjak2 lines G19 and H12 (n=2). Right: HUDEP-2 cells analyzed with the same antibody panel express much higher levels of CD34, 90 and 45, more consistent expression of CD117 and lower expression of CD235a. HUDEP-2 are blocked at an earlier stage of differentiation than the kitjak2 cells.

C: Romanowsky staining of the A4, H5, H12 and H12 SREs grown in DI conditions for about 100 days. Cells have very similar morphology during their self-renewing period. See figure S7 for micrograph of the A4 cells at an earlier passage.

**Figure S11: SRE differentiation**

A: H5 SREs grown in DI conditions were differentiated as described in Figure 5A and expression of CD36 and CD71 was analyzed by flow cytometry at days 3, 6, 9 and 11. Expression of CD36 and CD71 decrease over time.

B: Micrographs illustrating the morphology of differentiated H5 SREs at day 3, 5, 7 and 9. As expected from the FACS analysis, the cells exhibit the morphology of increasingly mature erythroid precursors.

C: Scatterplot illustrating the average ± S.D. (n=3) of cell growth and viability during A4 SREs differentiation assessed after acridine orange and propidium iodide staining.

D: Apoptosis analysis: differentiating A4 SREs were analyzed by FACS after staining with DAPI and annexin V-FITC. Bargraph illustrates the average ± S.D. (n=3) percentage of apoptotic cells at days 3, 5, 7 and 10.

E: Dotplots illustrating the expression of CD235a, CD43, CD36 and CD71 during A4 SREs differentiation. The pattern of differentiation of the A4 SREs is very similar to that of the H5 SREs.

**Figure S12: Apoptosis analysis**

Differentiating H5 SREs were analyzed by FACS after staining with DAPI and annexin V-FITC. Doplots illustrate the results. Data are summarized in Figure 5E.

**Figure S13: Late passage SRE differentiation**

A: Graphs illustrating the enucleation rates of the A4, H5, G19, H11 and H12 SREs observed at various passage numbers. SREs retain their ability to enucleate at a high rate even when close to senescence. The blue and green dots with a black outline were fed every two days during the differentiation.

B: Romanowsky stain illustrating the morphology of mature erythroid cells and cRetic obtained after 11 days of differentiation from early or late passage A4 SREs (top row). The two bottom rows illustrate the result of slightly larger scale differentiation experiments in which we purified the cRetics on day 11.

C: FACS analysis illustrating typical morphology (FSC-H and SSC-H) and draq5 analysis at the end of the differentiation.

**Figure S14: copy-number analysis by low-pass sequencing**

Genomic DNA was sequenced at a depth of 1 to 2 x and analyzed using the CNVkit software. Graphs illustrate that PB MNCs O1 and O2, passage 38-40 iPSC O1, A4, H5, H12, G19 (derived from iPSC O1), and passage 28 iPSCs O2 D816V exhibit no detectable copy number variants greater than 1Mb (the limit of detection for this read depth). By contrast, transformed cells, HUDEP-2 and K562 cells, cultured for a long period of time exhibit a high level of aneuploidy.

| ***IMIT*** |
|---|
| IMDM with 1mM Glutamine |
| Methyl-β-Cyclodextrin 0.1mg/mL |
| Trolox 50μM |
| Insulin 10μg/mL |
| Optiferrin 20 μg/mL |
| FeIII-EDTA 4μM |
| Gibco Lipids (1.5X) |
| Ethanolamine 0.01% |
| |
| ***R5*** |
| RPMI 1640 |
| L-ascorbic acid 220 μM |
| Insulin 10μg/mL |
| Optiferrin 20 μg/mL |
| FeIII-EDTA 4μM |

**Table S1:** Media composition

| Day 1 | 2 | 3 to 10 | 10 to 17 | 17 to 24 | 24-31 | 31 to 38 |
|---|---|---|---|---|---|---|
| **S1** | **S2** | **S3** | **STIF** | **SED** | **SER** | **SER 2** |
| Activin A 5ng/mL | Activin A 5ng/mL | | | | | |
| Inhibitor VIII 2µM | Inhibitor VIII 2µM | | | | | |
| Wnt3A/5A 5ng/mL each | Wnt3A/5A 5ng/mL each | | | | | |
| BMP4 10ng/mL | BMP4 20ng/mL | BMP4 20ng/mL | | | | |
| VEGF 10ng/mL | VEGF 30ng/mL | VEGF 30ng/mL | | | | |
| | b-Estradiol 0.4ng/mL | b-Estradiol 0.4ng/mL | | | | |
| | | SB431542 3µM day 3 only | | | | |
| | | Heparin 5µg/mL | Heparin 5µg/mL | | | |
| | | | GM-CSF 20 ng/mL day 17 only | | | |
| bFGF 10ng/mL | bFGF 10ng/mL | bFGF 20ng/mL | bFGF 5ng/mL | | | |
| | SCF 20ng/mL | SCF 30ng/mL | SCF 15ng/mL | SCF 100ng/mL | SCF 50ng/mL | SCF 10ng/mL |
| | | TPO 10ng/mL | TPO 10ng/mL | | | |
| | | IGF2 10ng/mL | IGF2 10ng/mL | | | |
| | | UM171* 30nM day 6 only | UM171* 30nM | | | |
| | | IBMX 50µM | IBMX 30µM | | | |
| | | | | EPO 4U/mL | EPO 4U/mL | EPO 4U/mL |
| | | | | Dex 1mM | | |
| | | *: UM171 can be replaced with 500nM UM729 | | | RU-486 1µM | RU-486 1µM |

**Table S2:** Supplements composition.

| Antibody | color | company | cat# |
|---|---|---|---|
| **CD11b** | PE-CY5 | Invitrogen | 15-0118-41 |
| **CD11c** | PE-CY5 | Biolegend | 301609 |
| **CD14** | PE-CY5 | Invitrogen | 15-0149-42 |
| **CD15** | PE-CY5 | Biolegend | 323013 |
| **CD16** | PE-CY5 | Biolegend | 302009 |
| **CD19** | PE-CY5 | ebioscience | 15-0199-42 |
| **CD56** | PE-CY5 | Invitrogen | 15-0567-42 |
| **CD123** | BV605 | Biolegend | 306026 |
| **CD36** | AF488 | Biolegend | 336232 |
| **CD71** | SB780 | Invitrogen | 78-0719-42 |
| **CD235A** | BV421 | BD | 562938 |
| **CD31** | BV805 | BD | 742013 |
| **CD34** | BUV563 | BC | 748740 |
| **CD38** | PE-CY7 | Invitrogen | 25-0389-42 |
| **CD43** | BUV395 | BD | 743616 |
| **CD45** | APC-Fire750 | Biolegend | 304062 |
| **CD45RA** | BV510 | BD | 563031 |
| **CD49f** | BV711 | BD | 740793 |
| **CD90** | PE/Daz-zle594 | Biolegend | 328134 |
| **CD117** | efluro450 | Biolegend | 313235 |
| **CD133** | BV480 | BD | 747837 |

**Table S3:** Antibody panel

| mutation | type | direction | sequence |
|---|---|---|---|
| **kit D816V** | sgRNA | antisense | 5'AGAATCATTCTTGATGTCTC |
| **jak2V617F** | sgRNA | sense | 5'AATTATGGAGTATGTGTCTG |
| **kitD816V mutated** | HDR donor | sense | 5'ACCTAATAGTGTATTCACAGAGACTTGGCAGCCAGAAA-TATCCTCCTTACTCATGGTCG-GATCACAAAGATTTGTGATTTTGGTCTAGCGAGAGTGATCAAGAATGATTCTAATTATGTGGTTAAAGGAAACGTGAG-TACCCATTCTCTGCTTGACAGTCCTG-CAAAGGATTTTTAGTTTCAACTTTCGATAAAAATTGT |
| **kitD816VWT** | HDR Donor | sense | 5'ACCTAATAGTGTATTCACAGAGACTTGGCAGCCAGAAA-TATCCTCCTTACTCATGGTCG-GATCACAAAGATTTGTGATTTTGGTCTAGCGAGAGACATCAAGAATGATTCTAATTATGTGGTTAAAGGAAACGTGAG-TACCCATTCTCTGCTTGACAGTCCTG-CAAAGGATTTTTAGTTTCAACTTTCGATAAAAATTGT |
| **jak2V617F** | HDR donor | antisense | 5'CTGAATTTTCTATATAAACAAAAACAGATGCTCTGA-GAAAGGCATTAGAAAGCCTGTAG-TTTTACTTACTCTCGTCGCCGCAAAAGCAGACTCCATAATTTAAAACCAAATGCTTGTGAGAAAGCTTGCTCATCATACTT-GCTGCTTCAAAGAAA-GACTAAGGAAAAAAAAAAGTACAAAGAATTGTTGTTTGACTGTTG |

**Table S4:** Sequence of the sgRNA and HDR donor oligonucleotides used to generate the kitD816V and jak2V617F lines.

| Reagent | Provider | Catalog Number |
|---|---|---|
| IMDM with 1mM Glutamine | Biochrom | FG0465 |
| RPMI 1640 with 1mM Glutamine | Gibco | 61870 |
| StemSpan SFEM | StemCell Technologies | 09650 |
| Methyl-β-Cyclodextrin | Sigma | C4555 |
| Trolox | Sigma | 238813 |
| Insulin | Sigma | I9218 |
| Chemically defined Lipids 200X | Gibco | 11905 |
| Ethanolamine | Sigma | E0135 |
| L-ascorbic acid | Sigma | A8960 |
| Optiferrin | FisherScience | NC9954311 |
| FeIII-EDTA | Sigma | E6760 |
| BMP4 | R&D Systems/Biotechne | 314-BP |
| VEGF165 | Peprotech | 100-20 |
| Wnt3A | R&D Systems/Biotechne | 5036-WN |
| Wnt5A | R&D Systems/Biotechne | 645-WN |
| Activin A | Peprotech | 120-14 |
| GSK3β Inhibitor VIII | Calbiochem/EMD Millipore | 361549 |
| bFGF | Peprotech | 100-18B |
| SCF | Peprotech | 300-07 |
| β-Estradiol | Sigma | E2758 |
| TPO | Peprotech | 300-18 |
| IGF1 | Alfa Aesar | BT-106 |
| IGF2 | Alfa Aesar | BT-107 |
| SB431542 | Tocris/Biotechne | 1614 |
| UM171 | Stemcell Technologies | 72912 |
| IBMX | Sigma | I5879 |
| PDGF AB | Peprotech | 100-00AB |
| ANGPTL5 | R&D Systems/Biotechne | 6675-AN |
| CCL28 | Peprotech | 300-57 |
| Heparin | Sigma | H3149 |
| EPO | Amgen | NDC 55513-126-10 |
| Dexamethasone | Sigma | D4902 |
| RU486 | Sigma | M8046 |
| FLT3L | Peprotech | 300-19 |
| GM-CSF | Peprotech | 300-23 |

**Table S5: Reagents**

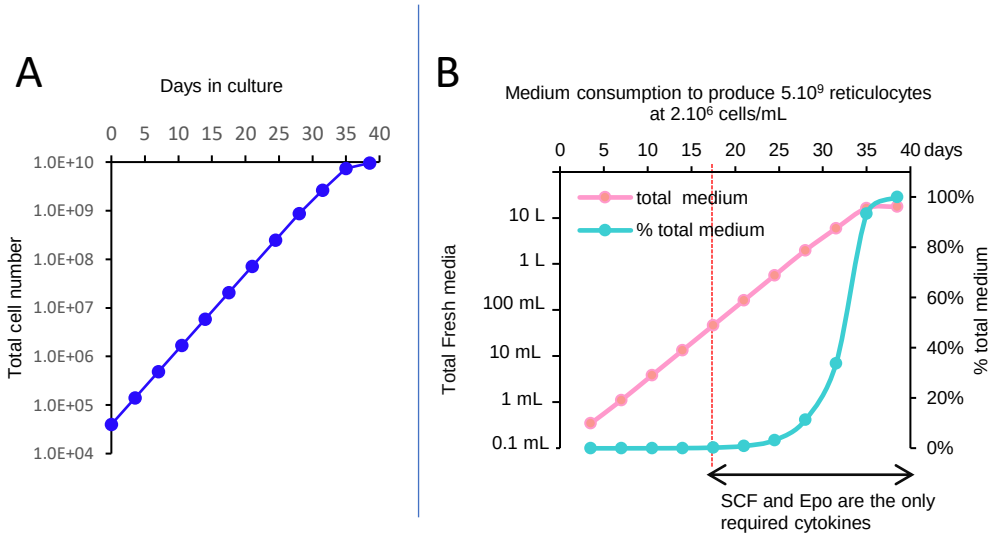
A
Days in culture
0 5 10 15 20 25 30 35 40
1.0E+10
1.0E+09
1.0E+08
1.0E+07
1.0E+06
1.0E+05
1.0E+04
Total cell number
B
Medium consumption to produce 5.10⁹ reticulocytes
at 2.10⁶ cells/mL
0 5 10 15 20 25 30 35 40 days
total medium
% total medium
10 L
1 L
100 mL
10 mL
1 mL
0.1 mL
Total Fresh media
100%
80%
60%
40%
20%
0%
% total medium
SCF and Epo are the only
required cytokines

Figure S1

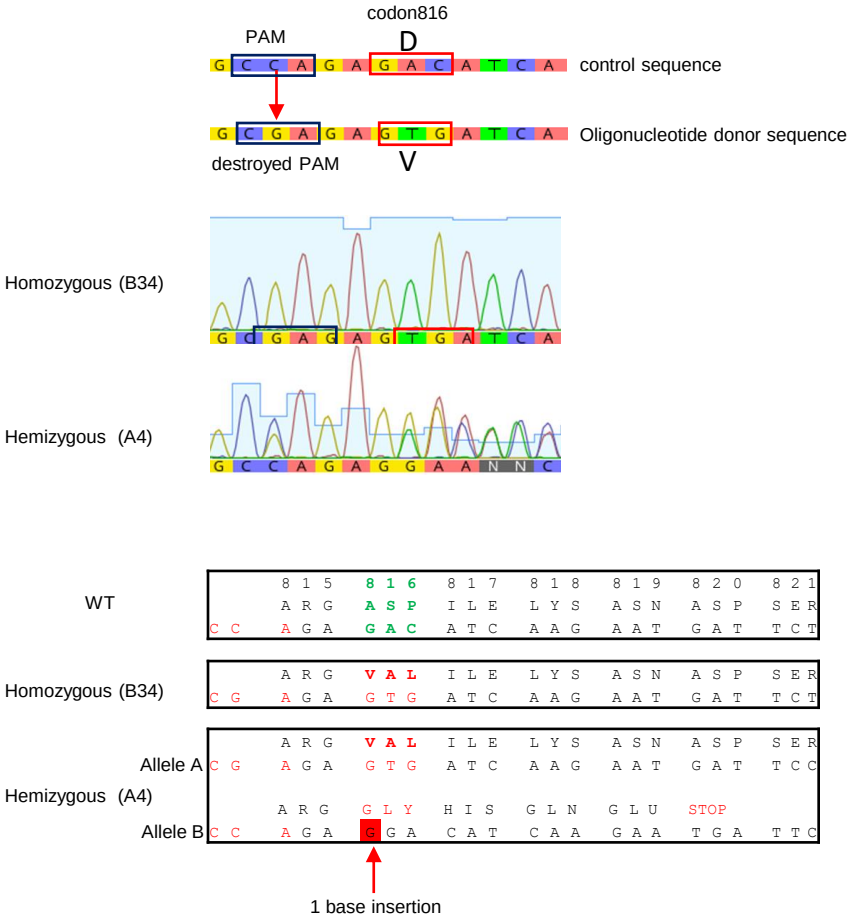
codon816
PAM
D
control sequence
Oligonucleotide donor sequence
destroyed PAM
V
Homozygous (B34)
Hemizygous (A4)
WT
Homozygous (B34)
Allele A
Hemizygous (A4)
Allele B
1 base insertion

Figure S2

# Wildtype (donor O1)

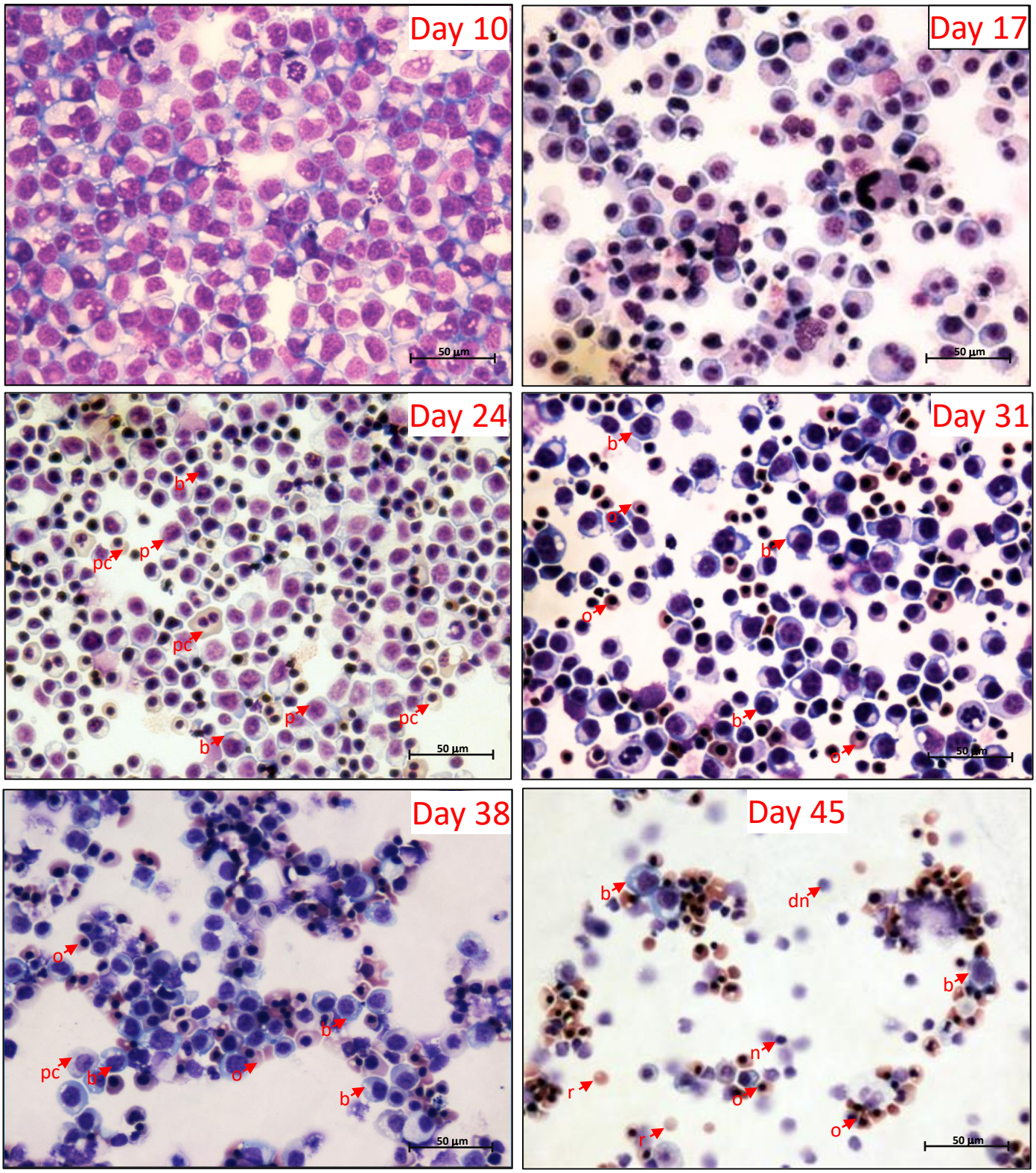


r = reticulocyte o = orthochromatic E pc= polychromatic E

b= basophilic E b= pro E n= nucleus dn= dead nucleus

Figure S3A

# A4 (D816V) hemizygous

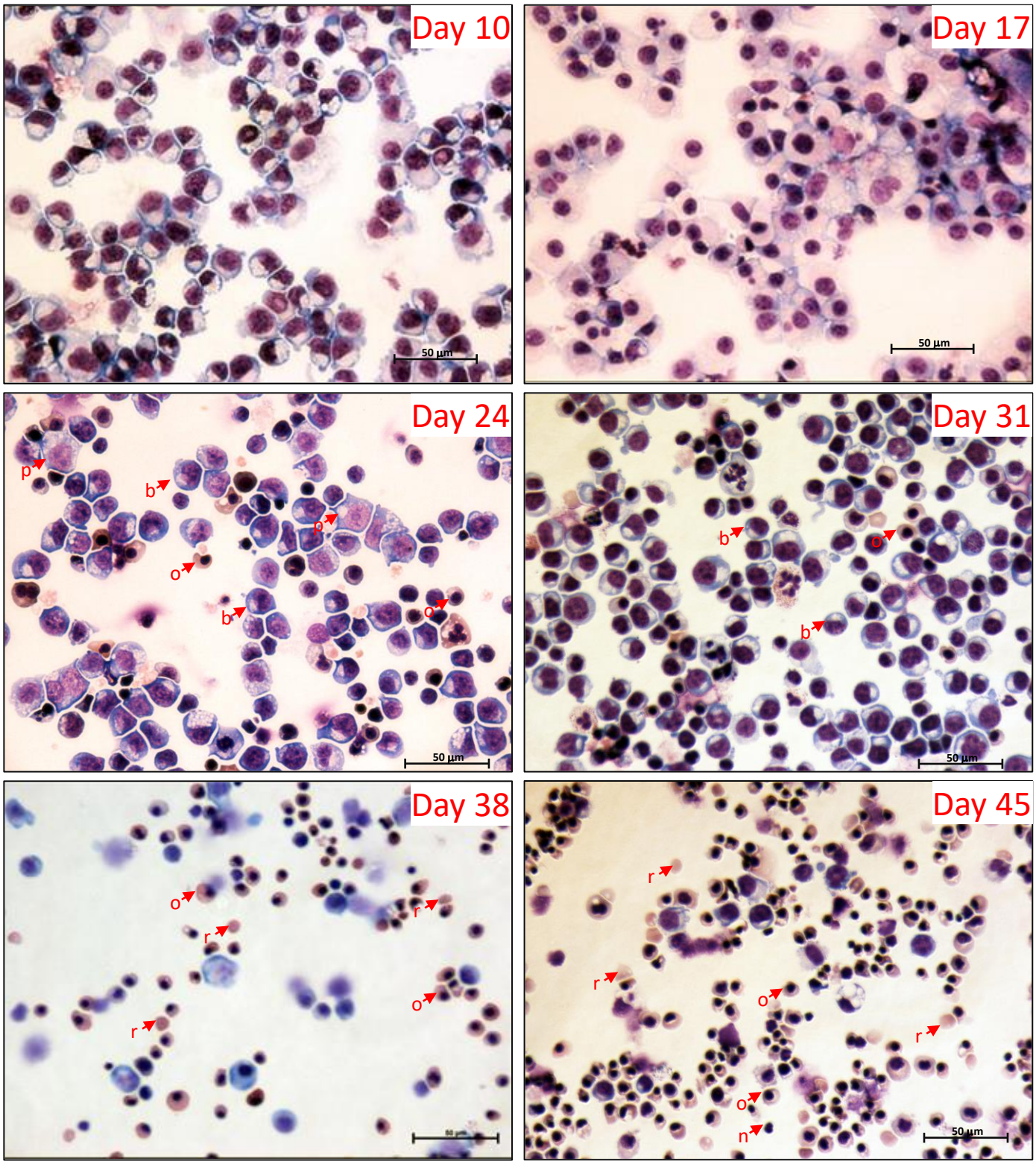


r = reticulocyte  o = orthochromatic E  pc= polychromatic E
b= basophilic E  b= pro E  n= nucleus  dn= dead nucleus

Figure S3B

# B4 (D816V) homozygous

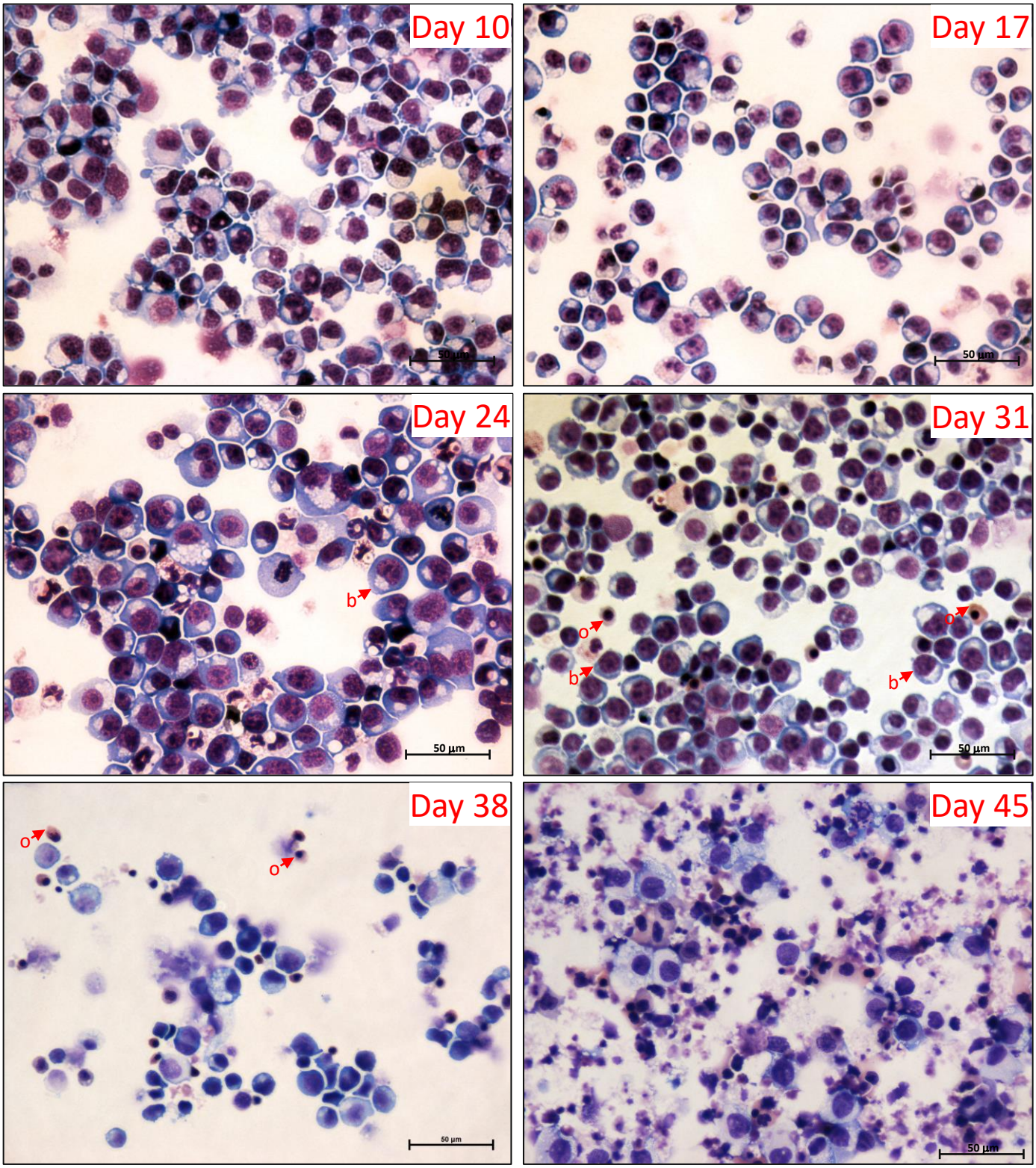


r = reticulocyte  o = orthochromatic E  pc= polychromatic E
b= basophilic E  b= pro E  n= nucleus  dn= dead nucleus

Figure S3C

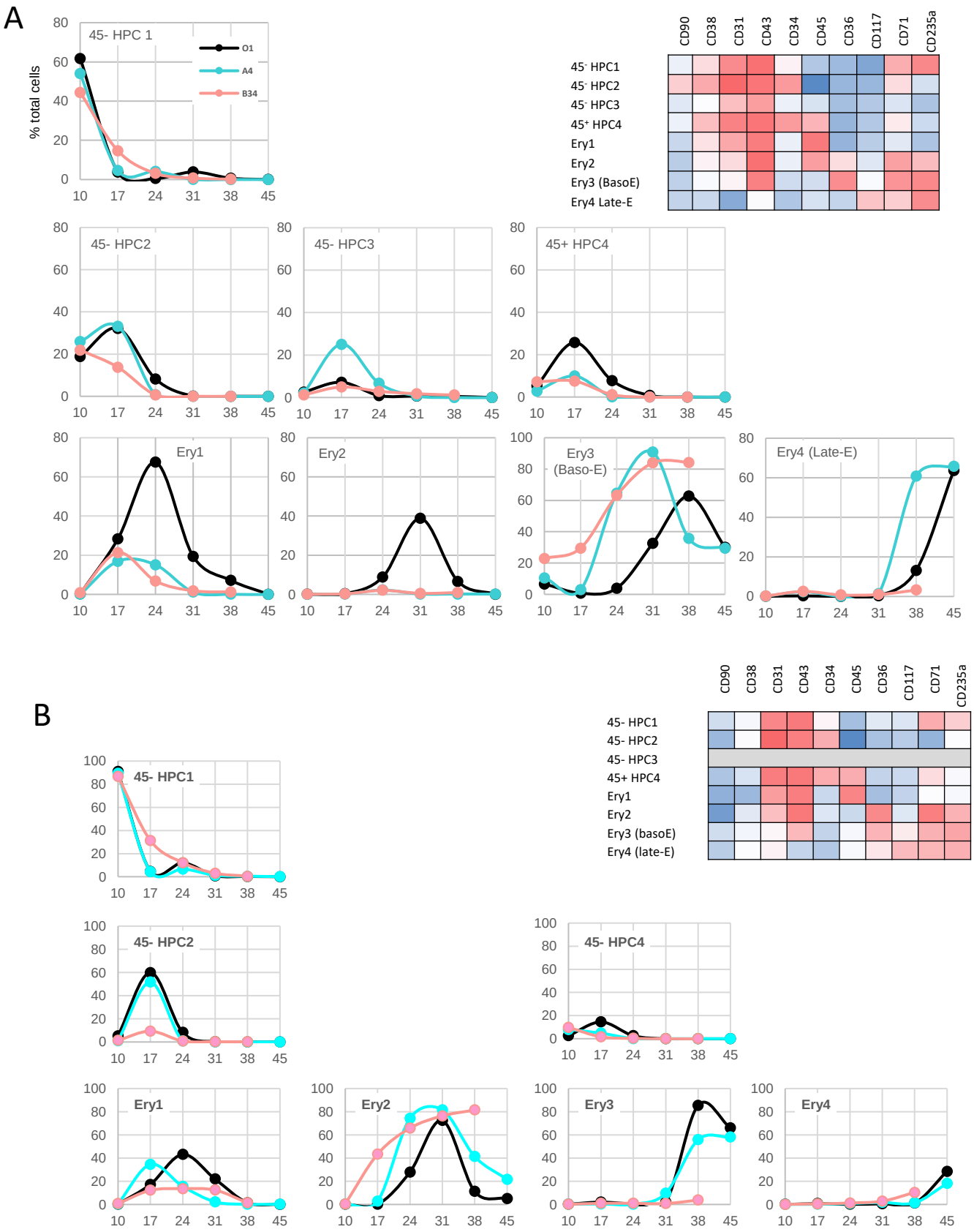
A
% total cells
45- HPC 1
O1
A4
B34
CD90
CD38
CD31
CD43
CD34
CD45
CD36
CD117
CD71
CD235a
45- HPC1
45- HPC2
45- HPC3
45+ HPC4
Ery1
Ery2
Ery3 (BasoE)
Ery4 Late-E
45- HPC2
45- HPC3
45+ HPC4
Ery1
Ery2
Ery3
(Baso-E)
Ery4 (Late-E)
B
45- HPC1
45- HPC2
45- HPC3
45+ HPC4
Ery1
Ery2
Ery3 (basoE)
Ery4 (late-E)
45- HPC4
Ery3
Ery4

Figure S4

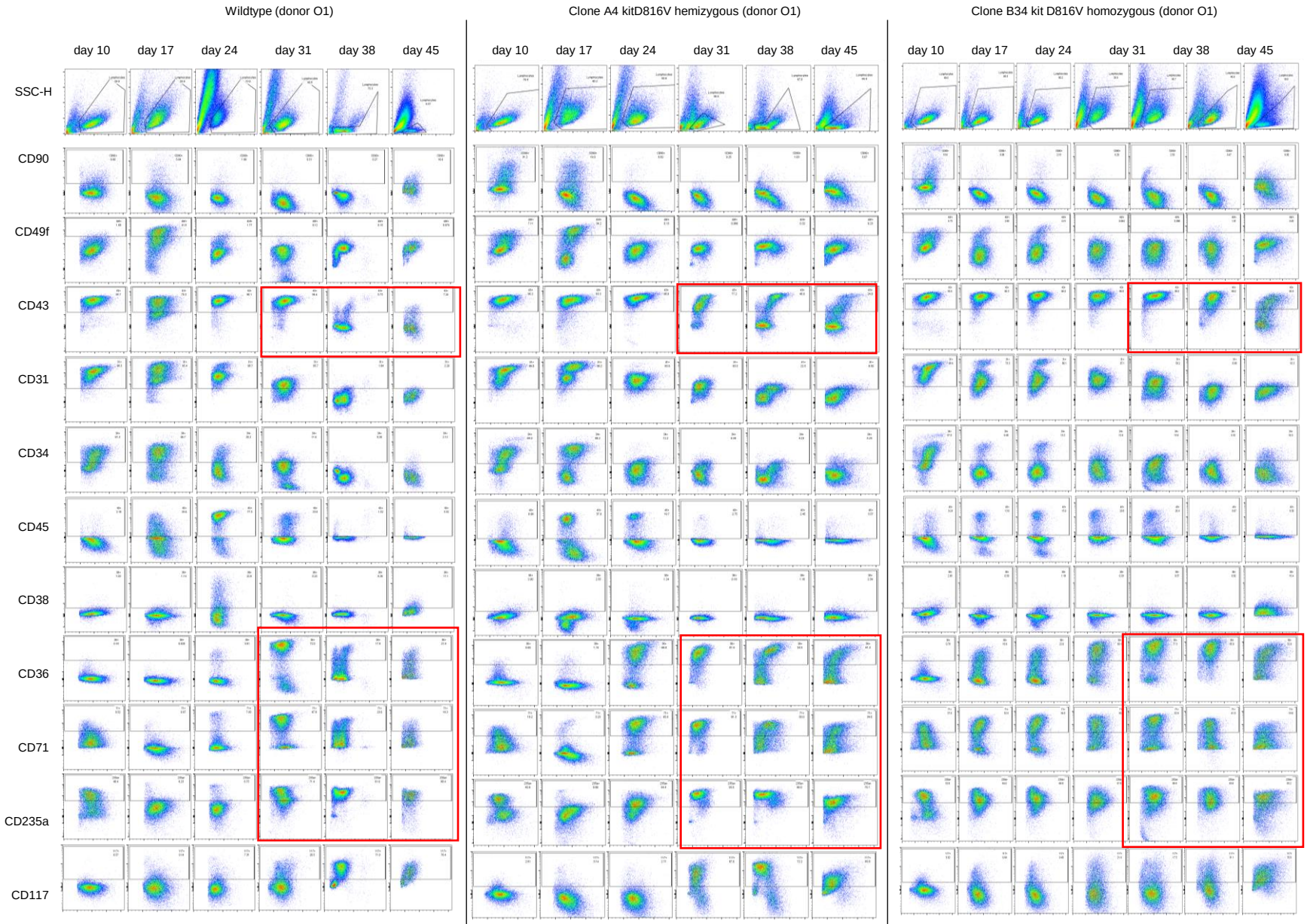
Wildtype (donor O1)
Clone A4 kitD816V hemizygous (donor O1)
Clone B34 kit D816V homozygous (donor O1)
day 10
day 17
day 24
day 31
day 38
day 45
SSC-H
CD90
CD49f
CD43
CD31
CD34
CD45
CD38
CD36
CD71
CD235a
CD117
FSC-H

Figure S4C

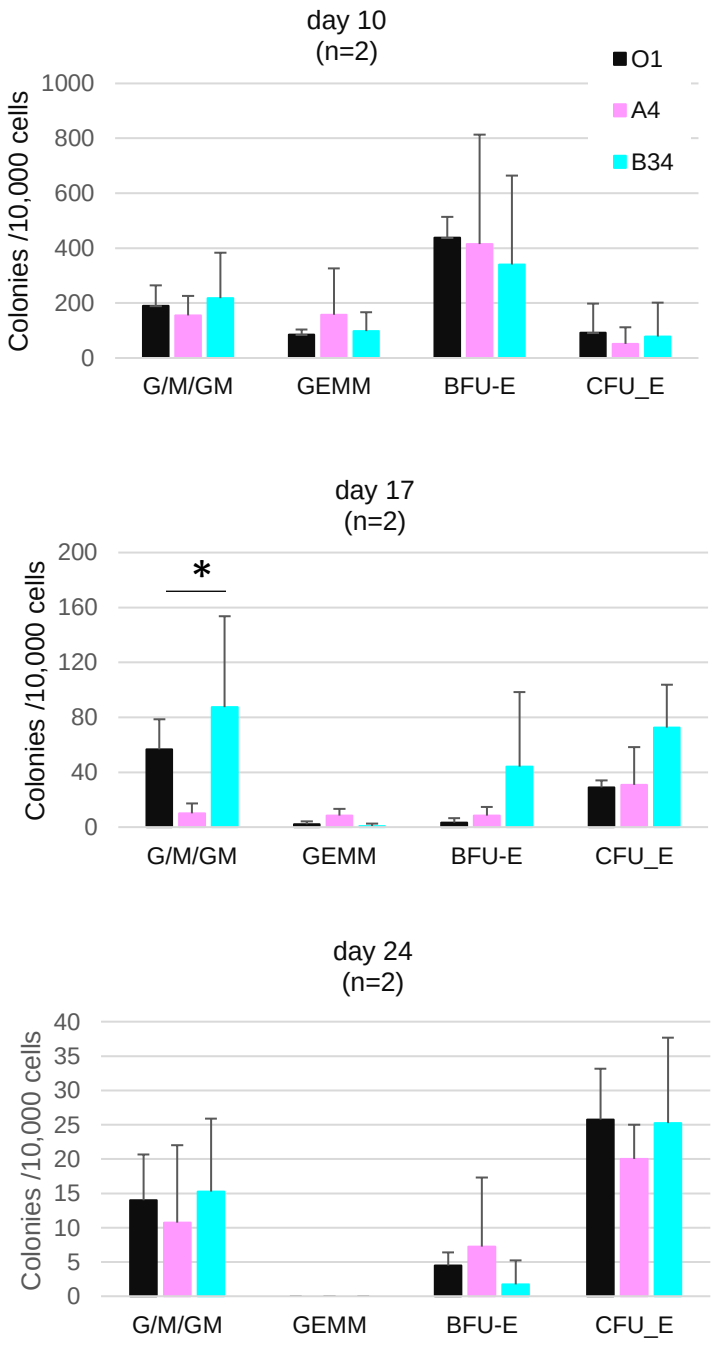
day 10
(n=2)
O1
A4
B34
Colonies /10,000 cells
1000
800
600
400
200
0
G/M/GM
GEMM
BFU-E
CFU_E
day 17
(n=2)
*
Colonies /10,000 cells
200
160
120
80
40
0
G/M/GM
GEMM
BFU-E
CFU_E
day 24
(n=2)
Colonies /10,000 cells
40
35
30
25
20
15
10
5
0
G/M/GM
GEMM
BFU-E
CFU_E

Figure S5

A

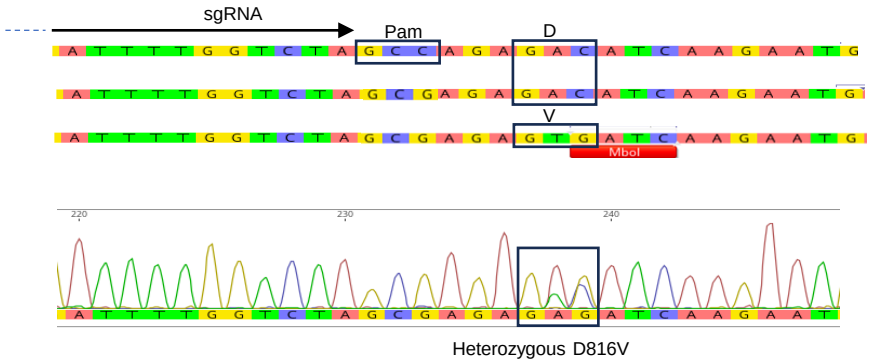


B

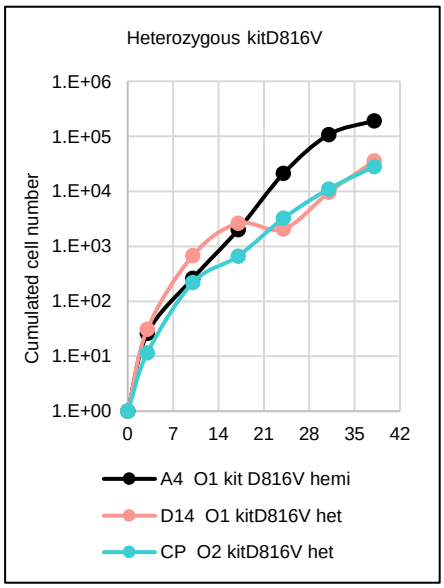


C

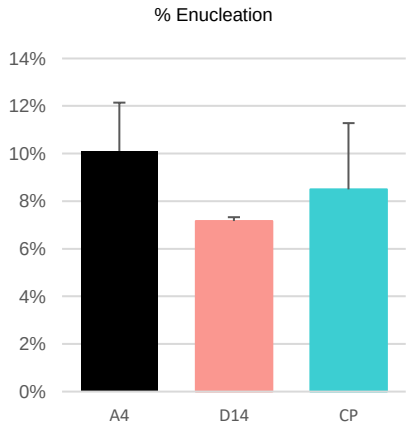


Figure S6

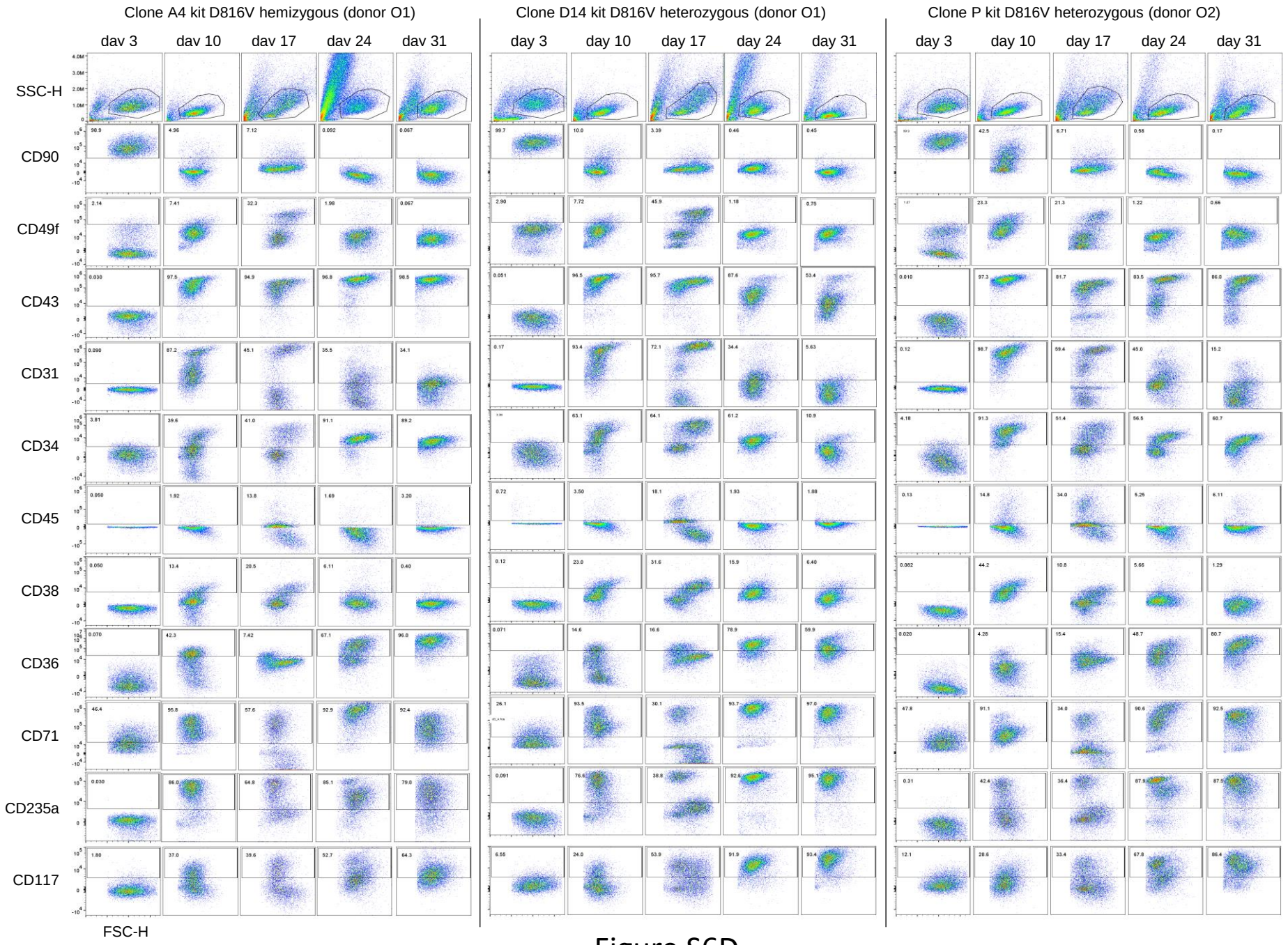
Clone A4 kit D816V hemizygous (donor O1)
Clone D14 kit D816V heterozygous (donor O1)
Clone P kit D816V heterozygous (donor O2)
day 3
day 10
day 17
day 24
day 31
SSC-H
CD90
CD49f
CD43
CD31
CD34
CD45
CD38
CD36
CD71
CD235a
CD117
FSC-H

Figure S6D

A

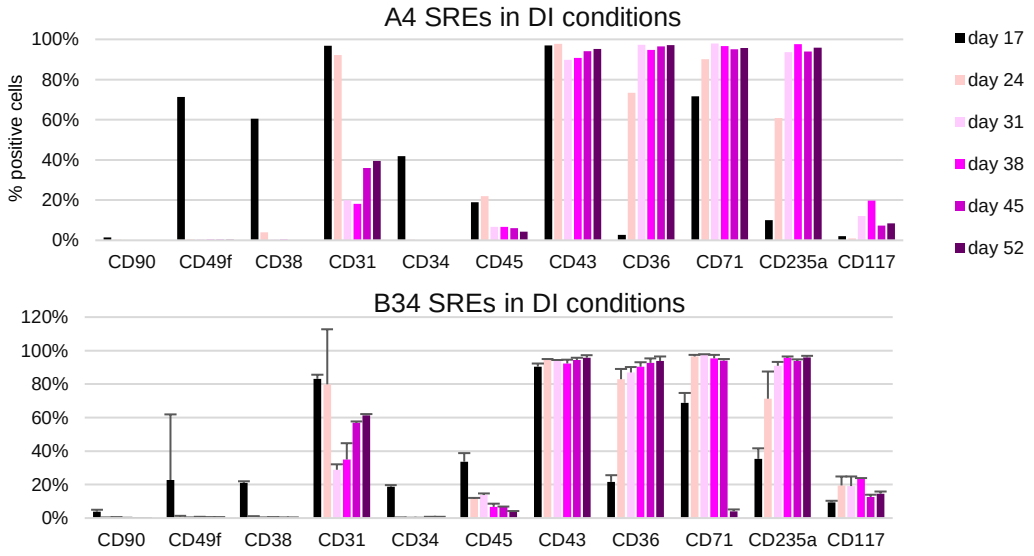


B

| days | protocol | 1 | 2 | 3-10 | 10-17 | 17-24 | 24-31 | 31-38 | 38 ..... |
|---|---|---|---|---|---|---|---|---|---|
| No SCF no EPO | PSC-RED | S1 | S2* | S3* | TIF | DI | R | R2 | |
| No Epo No SCF | SRE | S1 | S2* | S3* | TIF | DI | | | |

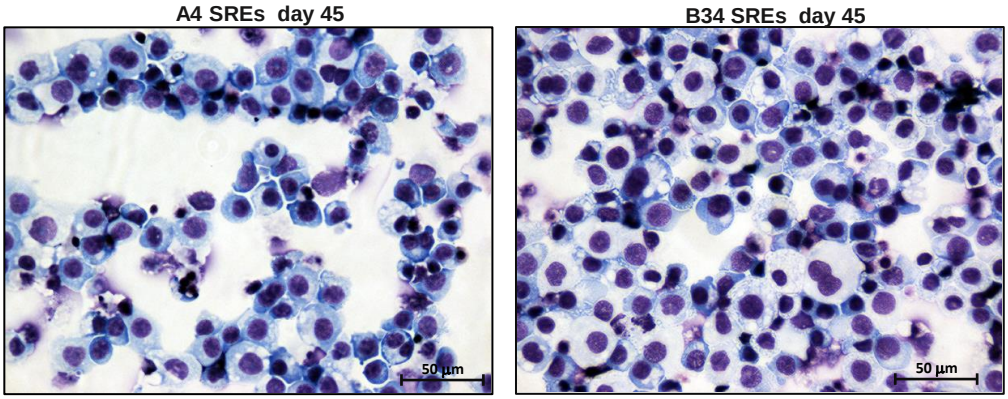


Figure S7

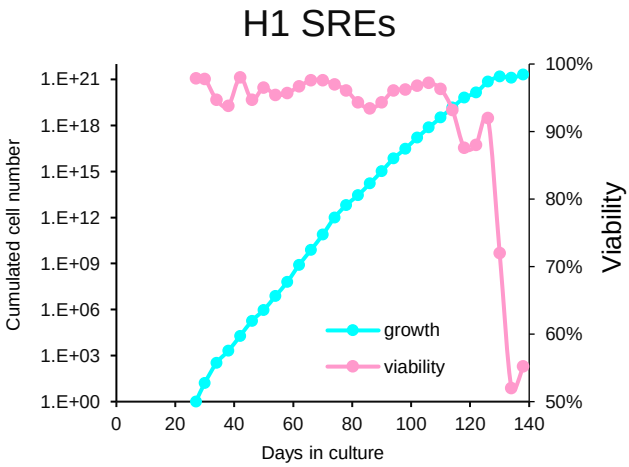
H1 SREs
Cumulated cell number
1.E+21
1.E+18
1.E+15
1.E+12
1.E+09
1.E+06
1.E+03
1.E+00
0
20
40
60
80
100
120
140
Days in culture
100%
90%
80%
70%
60%
50%
Viability
growth
viability

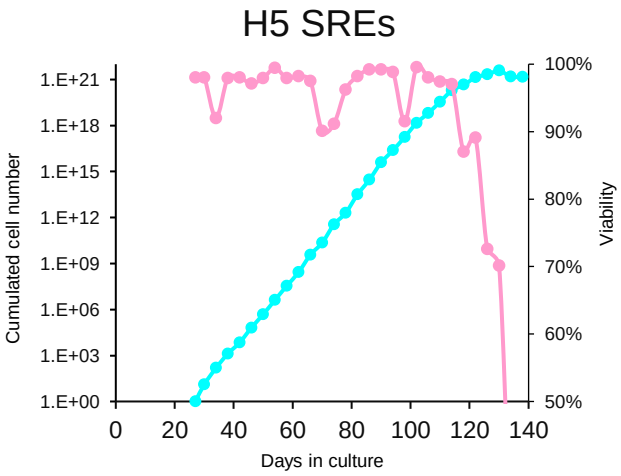
H5 SREs
Cumulated cell number
1.E+21
1.E+18
1.E+15
1.E+12
1.E+09
1.E+06
1.E+03
1.E+00
0
20
40
60
80
100
120
140
Days in culture
100%
90%
80%
70%
60%
50%
Viability

Figure S8

A

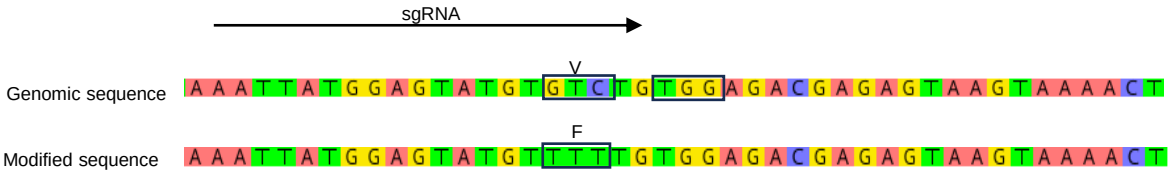


B

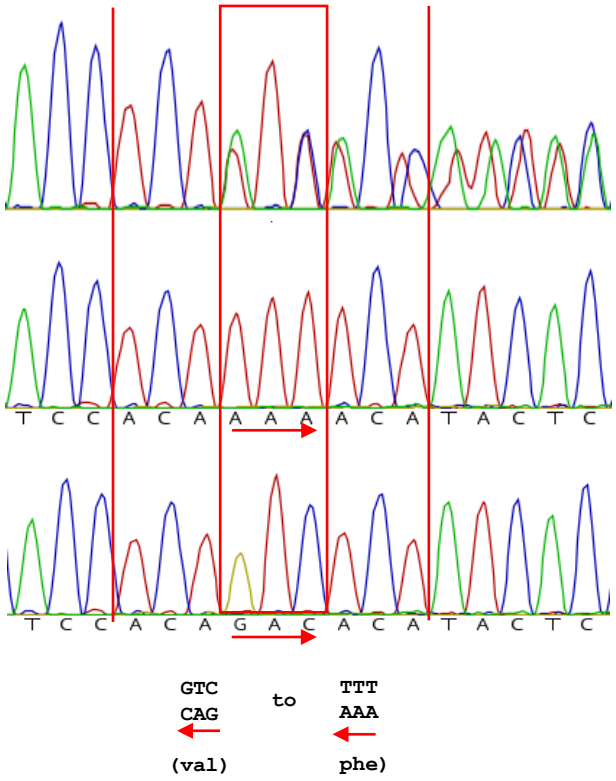


H5 (hemizygous jak2 657F)
jak2 del (656-657)

H12 (homozygous jak2 657F)

A4 (homozygous jak2 657V)

Figure S9

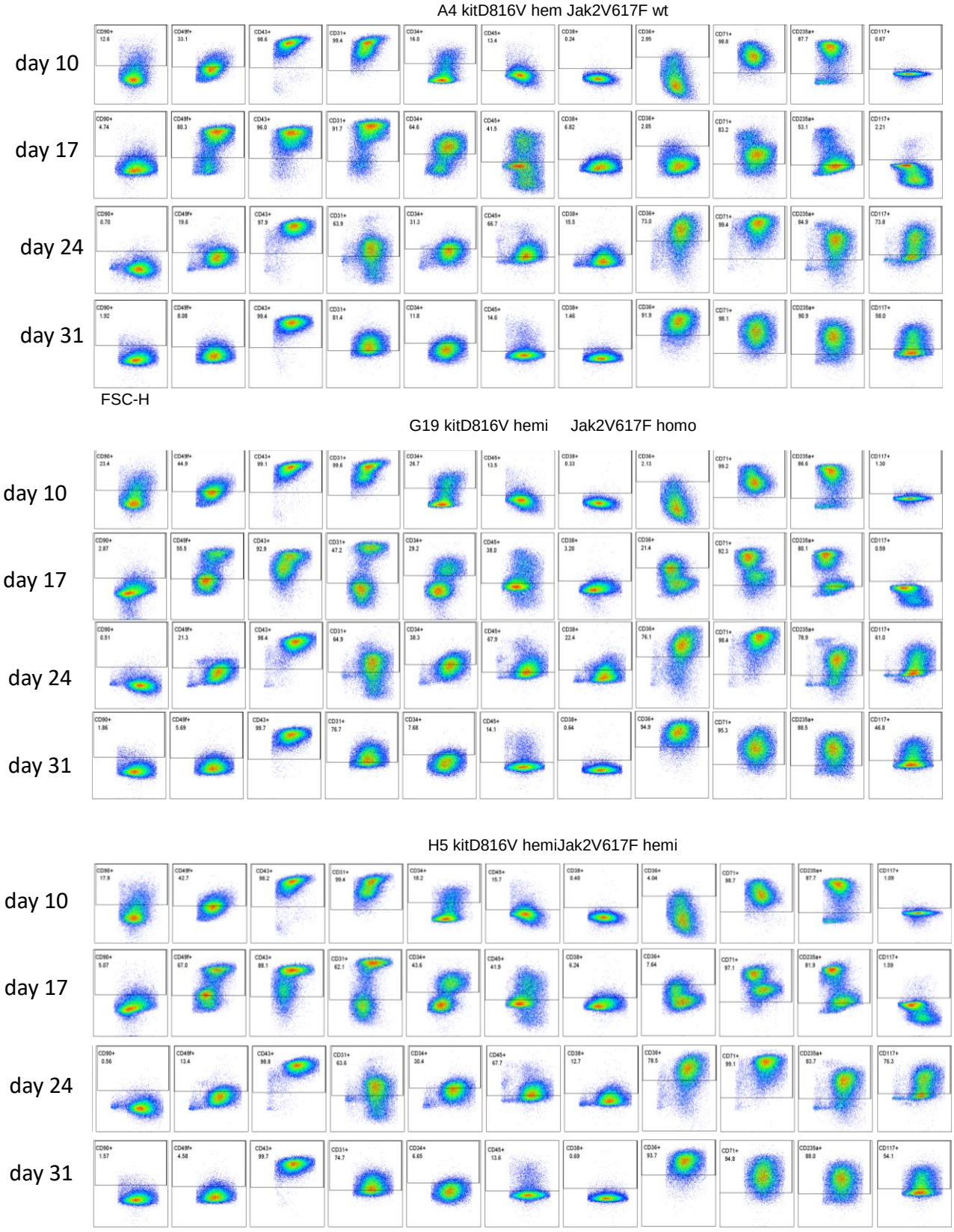
A4 kitD816V hem Jak2V617F wt
day 10
day 17
day 24
day 31
FSC-H
G19 kitD816V hemi Jak2V617F homo
day 10
day 17
day 24
day 31
H5 kitD816V hemiJak2V617F hemi
day 10
day 17
day 24
day 31

Figure S9C

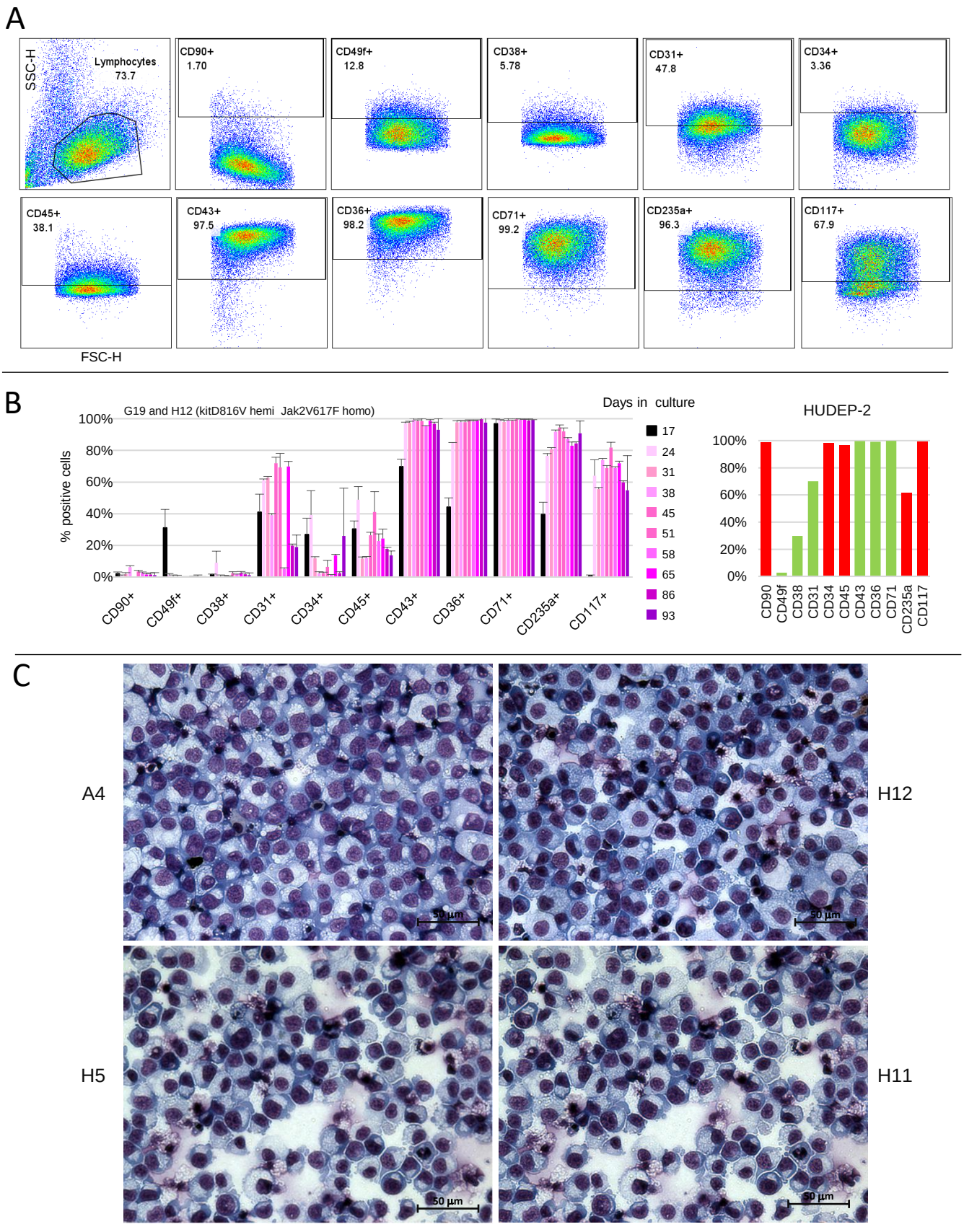
A
SSC-H
Lymphocytes
73.7
CD90+
1.70
CD49f+
12.8
CD38+
5.78
CD31+
47.8
CD34+
3.36
CD45+
38.1
CD43+
97.5
CD36+
98.2
CD71+
99.2
CD235a+
96.3
CD117+
67.9
FSC-H
B
G19 and H12 (kitD816V hemi Jak2V617F homo)
% positive cells
100%
80%
60%
40%
20%
0%
CD90+
CD49f+
CD38+
CD31+
CD34+
CD45+
CD43+
CD36+
CD71+
CD235a+
CD117+
Days in culture
17
24
31
38
45
51
58
65
86
93
HUDEP-2
CD90
CD49f
CD38
CD31
CD34
CD45
CD43
CD36
CD71
CD235a
CD117
C
A4
H12
H5
H11
50 µm

Figure S10

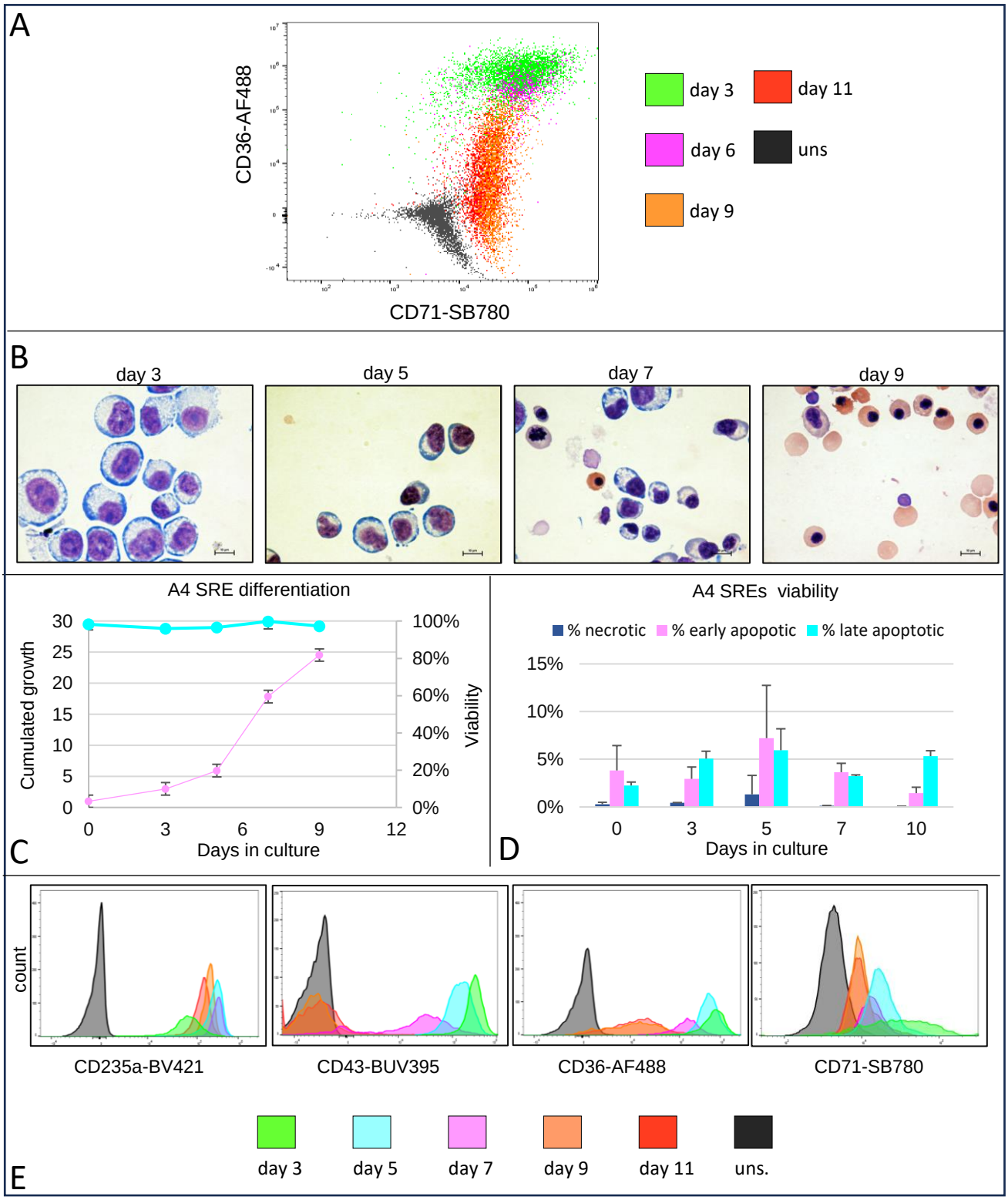
A
CD36-AF488
CD71-SB780
day 3
day 6
day 9
day 11
uns
B
day 3
day 5
day 7
day 9
A4 SRE differentiation
Cumulated growth
Viability
Days in culture
C
A4 SREs viability
% necrotic
% early apopotic
% late apoptotic
Days in culture
D
count
CD235a-BV421
CD43-BUV395
CD36-AF488
CD71-SB780
day 3
day 5
day 7
day 9
day 11
uns.
E

Figure S11

# Apoptosis analysis

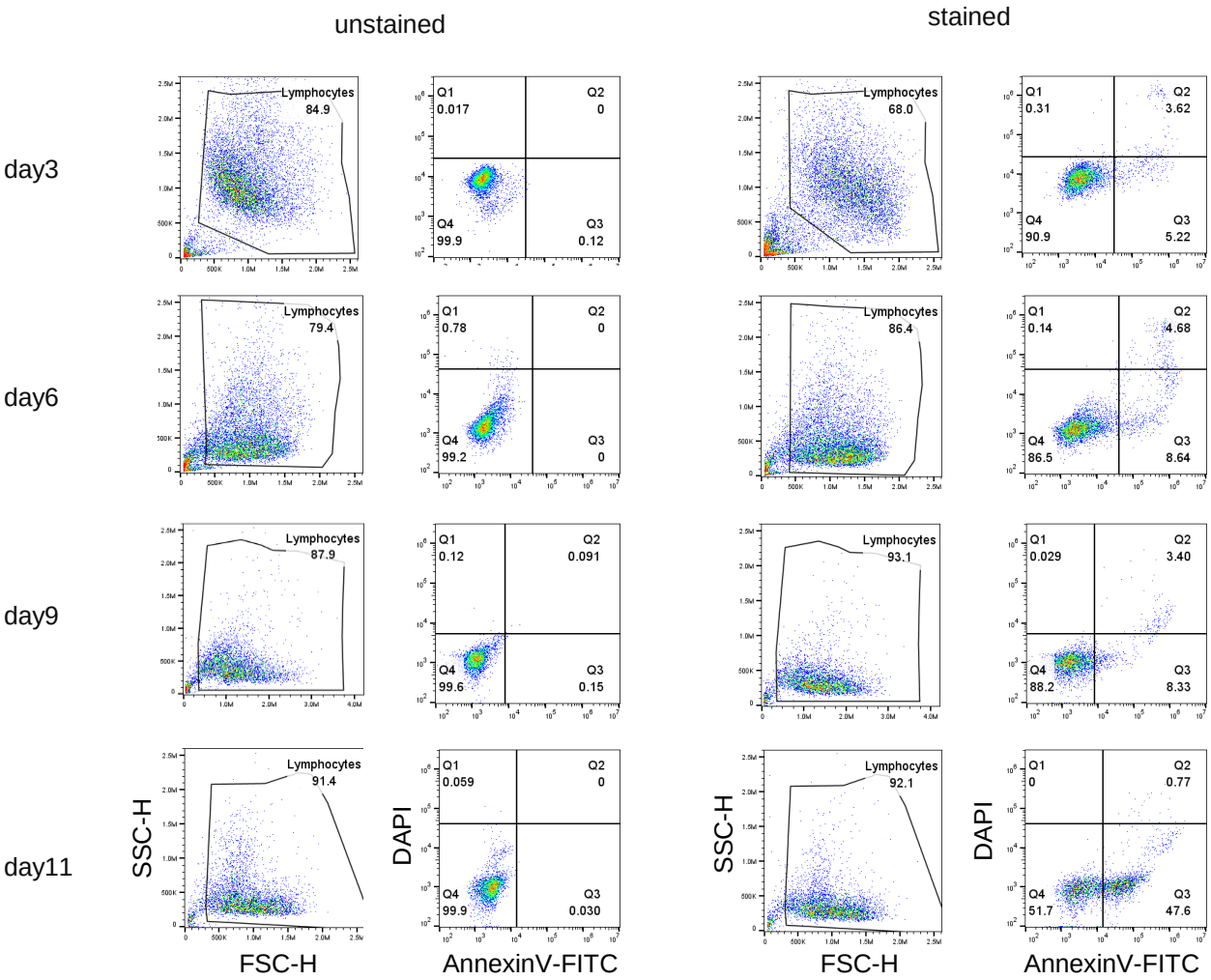


Figure S12

A

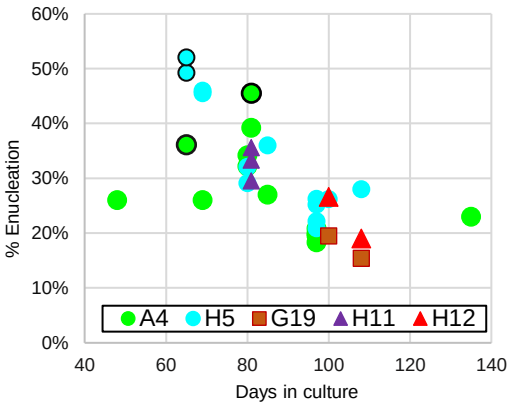


B

Early passage A4 SREs (day48)
after 7 days of differentiation (40x)

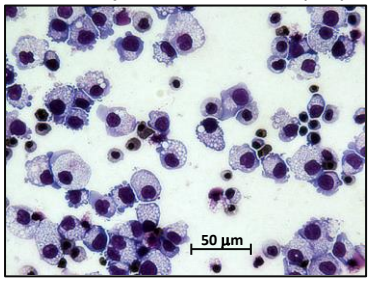


Early passage A4 SREs (day48)
after 10 days of differentiation (40x)

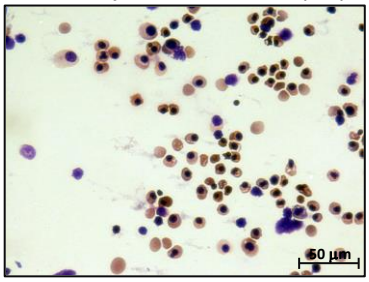


Late passage A4 SREs (day 135)
after 10 days of differentiation (40x)

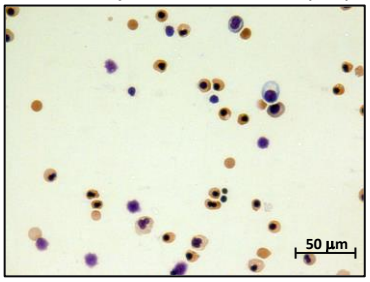


A4 SREs (day 80)
after 10 days of differentiation (40x)

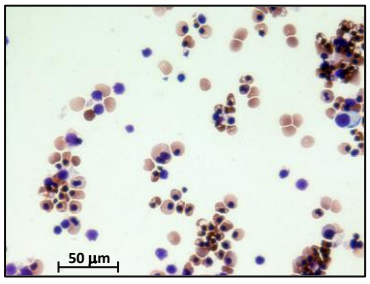


A4 SREs (day 80)
after 10 days of differentiation (100x)

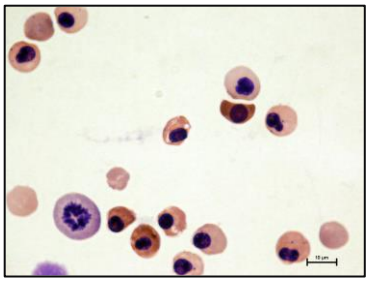

A4 SREs (day 80)
Purified cRetic (40x)

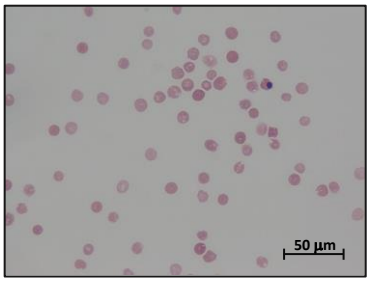


H5 SREs (day 80)
after 10 days of differentiation (40x)

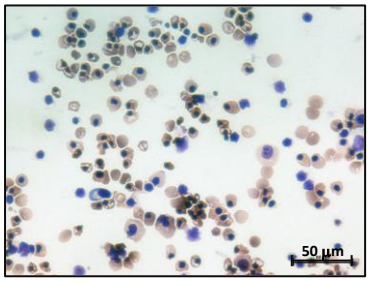


H5 SREs (day 80)
after 10 days of differentiation (100x)

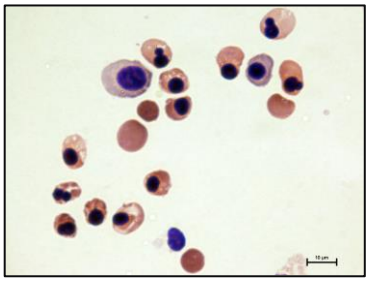

H5 SREs (day 80)
Purified cRetic (100x)

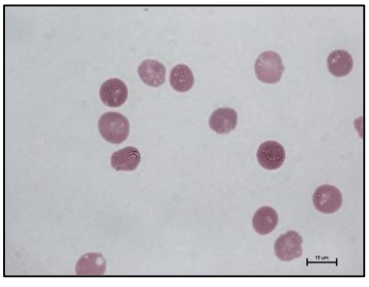

C

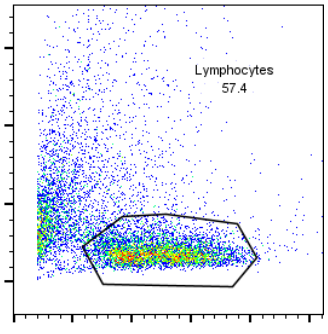


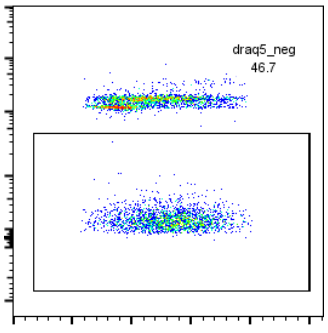


Figure S13

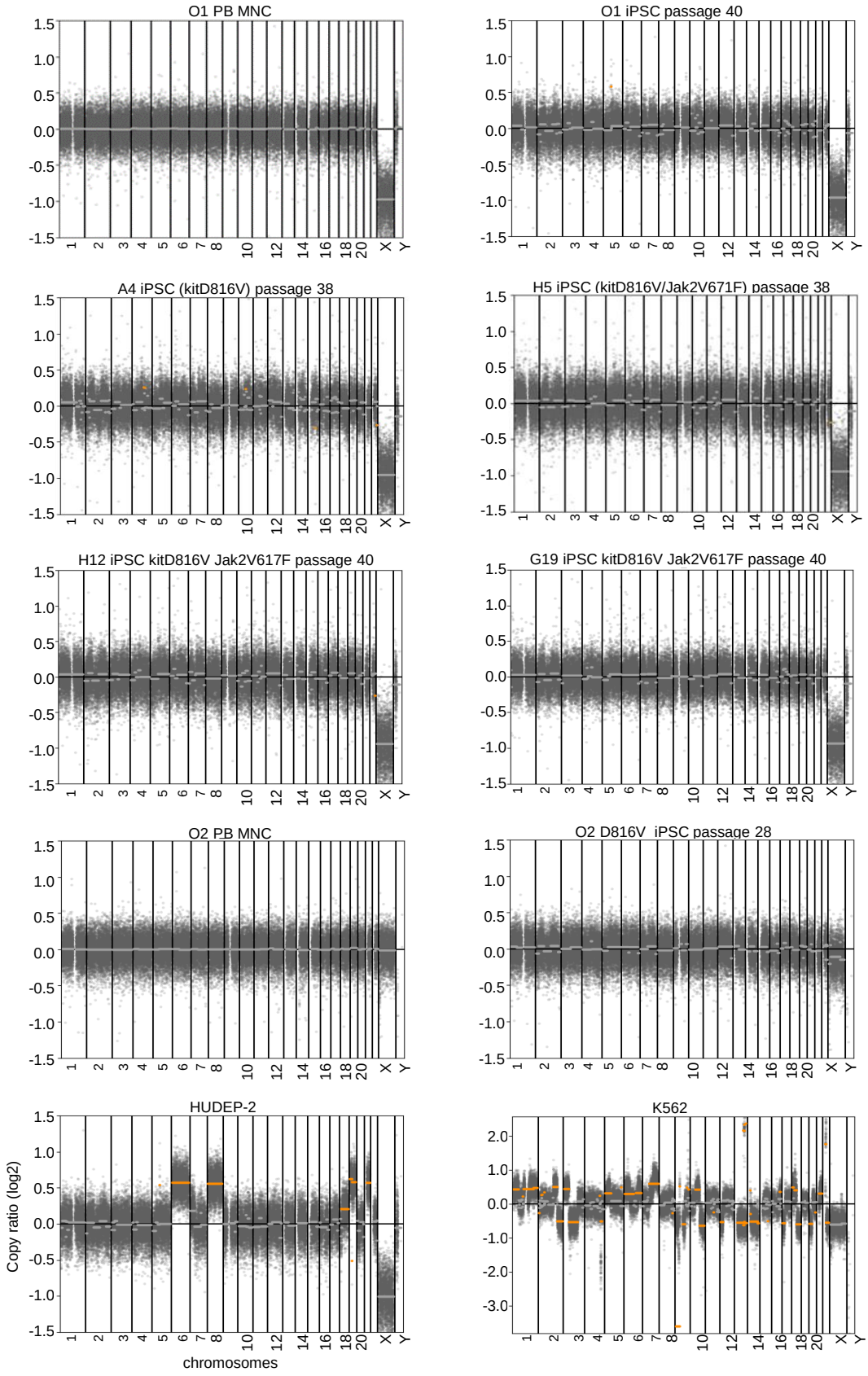
O1 PB MNC
O1 iPSC passage 40
A4 iPSC (kitD816V) passage 38
H5 iPSC (kitD816V/Jak2V671F) passage 38
H12 iPSC kitD816V Jak2V617F passage 40
G19 iPSC kitD816V Jak2V617F passage 40
O2 PB MNC
O2 D816V iPSC passage 28
HUDEP-2
K562
Copy ratio (log2)
chromosomes

Figure S14